Molecular Mechanisms of MMP9 Expression in Astrocytes Induced by Heme and Iron

The thesis presented to

The Faculty of Graduate and Post-Doctoral Studies

Of

University of Ottawa

By Mohamed Shaad Hasim

In partial fulfillment of the requirements for

Master Degree of Science in Cellular and Molecular Medicine

CMM Graduate Program

University of Ottawa

November 2012

Thesis Advisor

Dr. Wandong Zhang

Abstract

The disruption of the blood-brain barrier (BBB) occurs after ischemic and hemorrhagic stroke and contributes to secondary brain damage. Matrix metalloproteinase-9 (MMP9) has been identified to be the main mediator of post-stroke BBB disruption. It is unknown whether deposition of heme/iron in the brain following stroke would affect MMP9 expression. In this study, I have demonstrated that heme/iron up-regulated MMP9 expression in rat astrocytes and that this upregulation was most likely due to reactive oxygen species (ROS) generated by heme/iron deposition on cells. ROS can activate AP-1 and NFκB signaling pathways which were responsible for increased MMP9 expression. Inhibiting AP-1 and NFκB decreased MMP9 expression. Heme/iron deposition also activated Nrf-2 and increased the expression of neuroprotective heme oxygenase-1. My study suggests that heme and iron deposition generates ROS and increases MMP9 expression through AP-1 and NFκB signaling pathways and that targeting these pathways or clearance of heme and iron may modulate MMP9 expression for reduced damage.

TABLE OF CONTENTS

LIST OF FIGURES

LIST OF TABLES

List of Abbreviations

AP-1	Activator Protein-1
BBB	Blood Brain Barrier
BSA	Bovine Serum Albumin
CO	Carbon Monoxide
DMEM	Dulbecco's Modified Eagle's Medium
ERK	Extracellular Signal Regulated Kinase
HO-1	Heme Oxygenase-1
HT	Hemorrhagic Transformation
IκB-α	Inhibitor of Kappa B
IKK	IκB Kinase
IL	Interleukin
ICH	Intracerebral Hemorrhage
JNK	c-Jun N-Terminal Kinase
Keap1	Kelch-like ECH-associated protein 1
MAPK	Mitogen Activated Protein Kinase
MCAO	Meddle Cerebral Artery Occlusion
MCP-1	Monocyte Chemoattractant Protein 1
MMP	Matirx Metalloproteinase
NFκB	Nuclear Factor Kappa B
NRA	Neonatal Rat Astrocytes
Nrf2	Nuclear Factor (Erythroid-Derived 2)-like 2
NVU	Neurovascular Unit

PCR	Polymerase Chain Reaction
RBA	Rat Brain Astrocytes
ROS	Reactive Oxygen Species
SOD1	Superoxide Dismutase 1
TCA	Trichloroacetic Acid
TIMP	Tissue Inhibitor of Metalloproteinases
TJ	Tight Junctions
TNFα	Tumour Necrosis Factor- α
tPA	Tissue Plasminogen Activator

Acknowledgements:

Thank you to Dr. Wandong Zhang for giving me the opportunity to train and pursue my graduate studies in his laboratory. I would also like to thank Drs. Mahmud Bani, and Qiao Li for being on my advisory committee and for providing valuable feedback and guidance on my project.

To the members of the Zhang lab (Evan, Dema, Michelle, Hong, and Debbie). Thank you for making my time at the NRC a very enjoyable one. A special thanks to Debbie for taking the time to teach and train me.

Lastly, I would like to thank my parents and brothers for their continuing and unwavering support. Your belief in me helped me through the difficult times during the past couple years. I cannot thank you enough.

This study was supported by research grants from Heart & Stroke Foundation of Ontario and CIHR to Dr. W. Zhang. The research work was conducted in the Institute for Biological Sciences at the National Research Council of Canada

CHAPTER 1: INTRODUCTION

Acute ischemic stroke is the third leading cause of death in industrialized countries and the most frequent cause of permanent disability in adults worldwide (Lakhan SE et al. 2009). Ischemic stroke occurs when blood flow is blocked (most commonly by a blood clot) from the brain resulting in the inability of oxygen and glucose to be delivered to brain cells. The lack of oxygen and glucose to brain cells can cause cell death and permanent brain damage. Additionally, it has been shown that following stroke there is an increase in blood-brain barrier (BBB) permeability, leading to increased inflammatory cell infiltration, edema, and secondary brain damage. BBB disruption may also lead to hemorrhagic transformation (HT). During hemorrhagic stroke or HT, damage to the blood vessel causes intracerebral bleeding to occur which deposits blood cells and allows the entry of blood-borne neurotoxic agents into the brain incurring further damage. Understanding the processes leading to ischemic brain injury and BBB disruption are current challenges in the field of cerebral ischemia.

Currently the only approved drug for the treatment of ischemic stroke is tissue plasminogen activator (tPA). tPA is the enzyme responsible for the activation of plasmin by cleaving the precursor protein plasminogen. Plasmin then functions to dissolve clots in order to restore blood flow. Unfortunately tPA has a short therapeutic window and must be administered within the first three hours of stroke onset. Additionally, there have been many consequences associated with tPA including the potential for hemorrhage, edema, and BBB injury (Lee SR et al. 2007; Pfefferkorn T, Rosenberg GA. 2003). Further insights into the mechanisms involved in cerebral ischemia/stroke and BBB

disruption may help lead to minimizing brain damage, promoting recovery and the development of new therapies.

1.1 The Blood-Brain Barrier

The BBB is a selective barrier formed by endothelial cells that line the cerebral capillaries along with closely associated astrocytic end-feet processes, perivascular neuronal innervations, and pericytes (Cecchelli R et al. 2007) and it protects against the entry of pathogens and neurotoxic agents into the brain from the blood stream (Hu Q et al. 2011). It is primarily formed by brain microvascular endothelial cells that are interconnected by tight junctions (TJ) and adherens junctions (Abbott NJ et al. 2010). The TJ proteins act as the primary barrier between brain cells and the blood (Yang Y and Rosenberg GA. 2011a). Major tight junction proteins are occludin and claudins. The endothelial cells are also supported by a basal lamina which is comprised of collagen, fibronectin, heparan sulfate, and laminin (Yang Y and Rosenberg GA. 2011a). Together the endothelial cells, astrocytes, pericytes, microglia and neurons comprise the neurovascular unit (NVU) (Figure 1). Each cell type making up the NVU plays an important role in maintaining the structure and functionality of the BBB and brain homeostasis. As previously mentioned endothelial cells form the primary barrier between the blood and the brain through closely joined tight and adherens junctions. The brain endothelial cells also play an important role in the transport of nutrients, receptor-mediated signaling, and leukocyte trafficking (Persidsky Y et al. 2006). Astrocytes interact with and influence the phenotype of the brain endothelial cells by promoting the formation of tight junctions

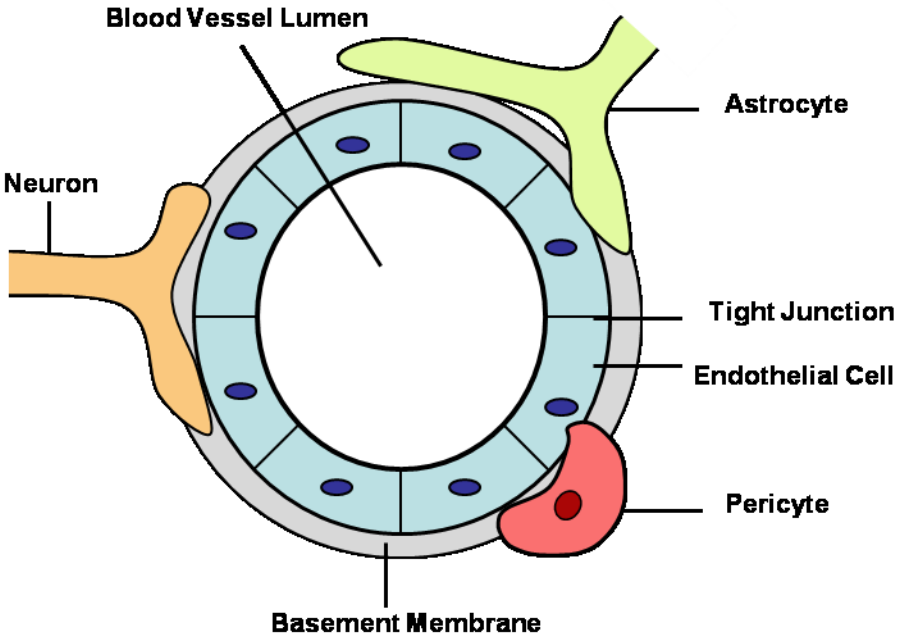

Figure 1: Schematic representation of the neurovascular unit (NVU).

The neurovascular unit is comprised of endothelial cells, astrocyte processes, pericytes, neurons and basement membrane. The endothelial cells line the cerebral microvessels and are tightly joined by tight and adherens junctions to help create the BBB, which is supported by the surrounding cells.

and reducing the area of the tight junctions (Tao-Cheng JH and Brightman MW 1988). They are also important for proper neuronal function (Abbot et al. 2006). Pericytes play an important role in maintaining the structure of the BBB (Persidsky Y et al. 2006). It has been shown that the lack of pericytes results in endothelial cell hyperplasia (Persidsky Y et al. 2006) and that pericytes promote endothelial cell differentiation and quiescence (Armulik A et al. 2005). Brain endothelial cells, astrocytes, and pericytes are also involved in the maintenance of the basement membrane that separates the brain endothelial cells from neighboring cells (Zlokovic BV 2008).

1.2 Matrix Metalloproteinase 9

Disruption of the BBB by degradation of its tight junctions, can lead to cell death, brain edema, hemorrhage, and leukocyte infiltration (Sandoval KE and Witt KA 2008). Following cerebral ischemia and ischemic or hemorrhagic stroke there is an opening of the BBB. This opening has been attributed to the upregulation of matrix metalloproteinase 9 (MMP9). MMP9 is a member of the matrix metalloprotease family. It is produced as a proenzyme (92 kDa) which is cleaved to become an activated enzyme of 85kDa. These enzymes are involved in processes such as tissue remodeling, wound healing, and angiogenesis (Sternlicht MD and Werb Z 2001). MMPs are either secreted or membrane bound and require proteolytic processing to become active (Cunningham LA et al. 2005). Due to MMP9's function it has also been sub-classified, along with MMP2, as gelatinase, enzymes that degrade denatured collagen and type IV collagen (Levicar N et al. 2003). MMP9 has also been characterized to degrade TJ proteins. Similar to the other members of the matrix metalloproteinase family, MMP9 consists of

hydrophobic pre-domain, an amino terminal prodomain, a Zn^{2+} binding domain, and hemopexin domain (Levicar N et al. 2003). MMP9 also contains three fibronectin type-II like modules in its catalytic domain which helps to mediate interactions with laminin, collagens, and gelatin (Tochowicz A et al. 2007; Xu X et al. 2005; Morgunova E et al. 1999; Collier IE et al. 1992). MMP9 is membrane bound or secreted (Cunningham LA et al. 2005). Once produced, MMP9 requires cleavage of the propeptide that closely interacts with its catalytic site in order to become activated (Elkins PA et al. 2002). This cleavage can occur through autoactivation or can be mediated by other activators such as proteases or reactive oxygen species (ROS) (Rajagopalan S et al. 1996). Following the cleavage of the pro-domain there is a conformational change called a cysteine switch which makes the catalytic Zn^{2+} available for the hydrolysis of the substrate, including TJ (Hu Q et al. 2011) and ECM proteins (Ram M et al. 2006).

In response to the elevated MMP9 present after cerebral ischemia, the tissue inhibitors of metalloproteinases -1 (TIMP-1) has been shown to be upregulated (Tsuge M et al. 2010). TIMPs are small glycoproteins that contain two domains, an N-terminal domain and a C-terminal domain which are each stabilized by three disulfide bonds (Williamson RA et al. 1990). They are the key inhibitors of MMPs in tissue. TIMPs inhibit MMPs by binding to the catalytic domain (Brew K et al. 2000). TIMP-1 is the primary TIMP responsible for the inhibition of MMP-9. Although the TIMPs demonstrate a preference for certain MMPs, they are still able to inhibit all other MMPs (Brew K et al. 2000). The expression of TIMP-1 was shown to occur through the MEK/ERK pathway in a rat middle cerebral artery occlusion (MCAO) model (Maddahi

A et al. 2009). Deletion of the TIMP-1 gene in mice caused an increase in MMP-9 expression and an increase in BBB permeability, apoptosis, and ischemic injury, demonstrating the important role of TIMP-1 after cerebral ischemia (Fujimoto M et al. 2008). Understanding the mechanisms of MMP-9 expression in response to ischemic stroke will allow for the identification of potential therapeutic targets for the development of treatment strategies.

1.3 MMP9 and BBB Disruption

Blood-brain barrier disruption has been observed to occur after a cerebral ischemic event. *In vivo* studies have shown that the disruption of the BBB results from upregulation of matrix metalloproteinases (MMP), specifically MMP9 which degrades the tight junctions, extracellular matrix, and basal lamina (Chen W et al. 2009; Hu Q et al. 2011; Yang Y and Rosenberg GA 2011b). In a rat model of transient MCAO, MMP9 activity was shown to co-localize with brain microvascular endothelial cells within the first 24 hours, but later (7-14 days) shifted and was mainly associated with astrocytes and neurons (Zhao BQ et al. 2006). The redistribution of MMP9 within the neurovascular unit suggests that it has a multiphasic role. In hypoxia/ischemia, it has been shown that MMP2 expression occurs first and leads to a reversible opening of the BBB (Yang Y et al. 2007). Following the first opening of the BBB, a second phase of opening occurs during which MMP9 expression is increased and results in more extensive damage of the BBB, supporting MMP9's dual role (Rosenberg GA et al. 1998). MMP2 and MMP9 knockout as well as MMP2/9 double knockout in mice has been shown to prevent hemorrhagic transformation following ischemia/reperfusion (Suofu Y et al. 2012).

Knockout of MMP9 was also shown to prevent degradation of the microvascular basal lamina following ischemia/reperfusion (Suofu Y et al. 2012). MMP9's role in the pathology of cerebral ischemia seems to be that it is first involved in BBB disruption, neuronal death, and hemorrhage, and is later involved in neurovascular remodeling during the repair phase after cerebral ischemia (Adibhatla RM and Hatcher JF 2008, Zhoa BQ et al. 2006, Cunningham LA et al. 2005). A protective effect against brain injury (Wang X 2000) and global/focal ischemia (Asahi M et al. 2001, Gidday JM et al. 2005, Lee SR et al. 2004) has been demonstrated in MMP9 knockout mice indicating the potential benefits of targeting MMP9 and associated signaling pathways for the treatment of cerebral ischemia.

1.4 Expression of MMP9

1.4.1 Neuroinflammation and MMP9

Neuroinflammation has been strongly correlated to the risk of cerebral ischemia, most commonly in stroke, as well as with the outcome from ischemic events (Denes A et al. 2010). Many inflammatory cytokines are expressed following cerebral ischemia, such as interleukin (IL)-1β, IL-6, IL-8, IL-10, monocyte chemoattractant protein-1 (MCP-1), and tumor necrosis factor- α (TNF-α) (Denes et al. 2010). The role of these cytokines has been greatly studied but a clear understanding of their roles in the progression of ischemic brain injury, and in terms of BBB disruption has not been fully established. Of the inflammatory cytokines elevated IL-1β and TNF-α have been shown to play prominent roles in the induction of MMP9 (Gottschall PE and Yu X 1995, Kaupipinen

TM and Swanson RA 2005, Crocker SJ et al. 2006). The most common pathways triggered are the MAPK/AP-1, and NF-κB pathways (Figure 2). The MAPK/AP-1 pathway involves the activation of a kinase cascade by a stimulus which binds to its receptor activating a small GTP-binding protein. This causes the activation of a MAPK kinase kinase (MAPKKK/MAP3K). The MAP3K phosphorylates and activates a MAPK kinase (MAPKK), which then activates the MAPK. The MAPK activates its target transcription factor. The NF-κB signaling pathway involves activation of IκB kinase (IKK) which phosphorylates IκB-α causing IκB-α degredation by the proteosome. IκB-α degradation relieves its inhibition of NF-κB and allows for its translocation to the nucleus where it becomes transcriptionally active. Oxidative stress and ROS can activate both MAPK-AP1 and NF-κB signaling pathways.

In vitro studies have shown the role of IL-1β in stimulating MMP-9 gene expression through various pathways. IL-1β was shown to induce MMP-9 expression and activity in A549 cells (human alveolar epithelial cell carcinoma) through the activation of MAPKs and the transcription factors AP-1 and NF-κB (Lin CC et al. 2009). The MAPKs activated in the A549 cells were p42/p44 MAPK, p38 MAPK, and JNK1/2. The activation of these MAPKs was found to be essential for IL-1β induced MMP-9 expression (Lin CC et al. 2009). IL-1β has also been shown to induce MMP-9 expression in RBA-1 cells (rat brain astrocytes) through the activation of MAPKs and NF-κB (Wu

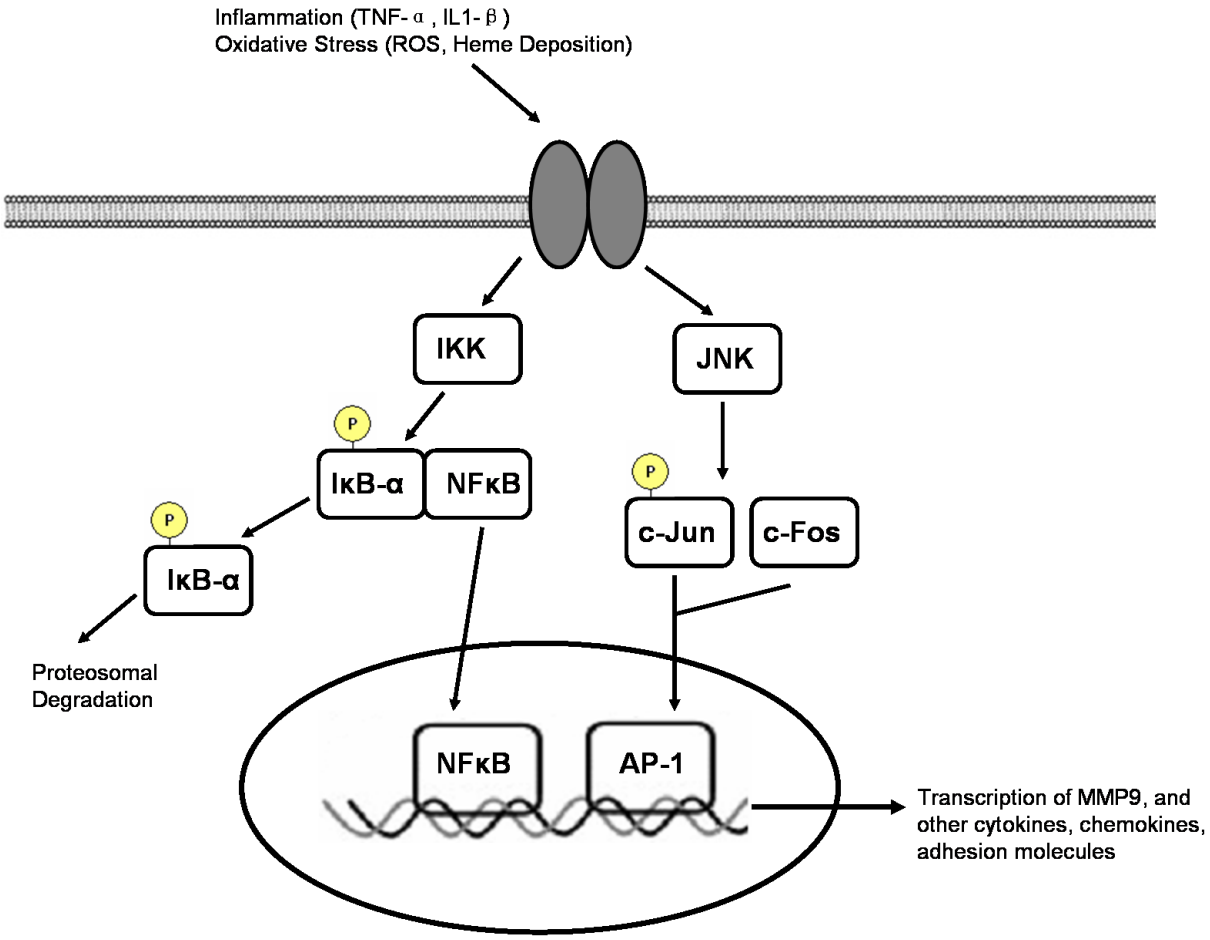

Figure 2. Stimulation of MMP9 Expression by Inflammatory Factors and Oxidative Stress.

Following cerebral ischemia there is an inflammatory response and the production of ROS. These stimulate the MAPK/AP-1 and NFκB signaling pathways resulting in the expression of MMP9.

CY et al. 2004). In this study the p42/p44 MAPK, p38 MAPK, and JNK were found to be essential for IL-1β induced MMP-9 expression in rat astrocytes (Wu CY et al. 2004).

Increased TNF-α has been linked to increases in BBB permeability and tight junction disruption (Lv S et al. 2010). TNF-α has also been shown to increase MMP-9 expression in cultured astrocytes and microglia (Gottschall PE and Yu X 1995,Kaupipinen TM and Swanson RA 2005, Crocker SJ et al. 2006). Direct injection of TNF-α into the brain of rats resulted in a significant increase in the expression and activation of MMP9 (Rosenberg GA et al. 1995, Candelario-Jalil E et al. 2007). Induction of MMP9, by TNF-α, has been shown to occur through the activation of NF-κB (Hozumi A et al. 2001, Itatsu K et al. 2009). TNF-α also induces MMP9 expression through the phosphorylation of extracellular signal-regulated kinase 1/2 (ERK1/2) and p38 MAPK after TNF-α interaction with TNF receptor 1 (TNFR1) (Itatsu et al. 2009). TNF-α has also been shown to stimulate other signaling pathways involved in MMP9 upregulation, including the PI3K/Akt pathway (Hwang MK et al. 2009), and MAPK/AP-1 pathway (Holvoet S et al. 2003).

MCP-1 has been identified to play a role in upregulating MMP9 following cerebral ischemia. MCP-1 plays a role in recruiting monocytes and macrophages to sites of inflammation within the brain. The inflammatory cells, such as neutrophils, express MMP9 and help to potentiate BBB breakdown (Rosell A et al. 2008; Gidday JM et al. 2005). In a transgenic mouse model that selectively overexpressed MCP-1, the mice exhibited larger infarct volumes following MCAO and the increase was associated with

increased recruitment and infiltration of inflammatory cells (Chen Y et al. 2003). The infiltration of inflammatory cells caused an increase in BBB breakdown and lead to increased neuronal damage following MCAO in mice. Additionally, when mice carrying leukocytes that did not express MMP9 underwent MCAO, they exhibited smaller infarcts (Gidday JM et al. 2005). Additionally, MCP-1 may also directly affect MMP9 expression through the activation of specific signaling pathways. It was shown that MCP-1 can cause an increase in MMP9 expression in human chondrosarcoma cells via the activation of NF-κB through a Ras/Raf/MEK/ERK signaling pathway (Tang CH and Tsai CC 2012).

1.4.2 Reactive Oxygen Species and MMP9

Reactive oxygen species (ROS) plays a role in the expression and activation of MMP9. During hypoxia/ischemia and reperfusion/reoxygenation, reactive oxygen species are generated. ROS exists in many forms including superoxide, hydroxyl radicals, and singlet oxygen. The overproduction of ROS leads to oxidative stress within the brain which can result in oxidative damage including cell death. This occurs due to the ROS oxidizing various cellular components such as DNA, proteins, and lipids (Gilgun-Sherki Y et al. 2001; Gorman AM et al. 1996; Simonian NA and Coyle JT 1996). ROS and oxidative stress may also play a role in regulating the activity and expression of MMPs. It has been shown that MMP9 can be activated by its nitrosylation by nitric oxide (Gu Z et al. 2002). This may also occur through oxidation by ROS. More likely is that ROS mediates MMP9 expression by acting on the redox sensitive elements of transcription

factors involved in MMP9 transcription, such as AP-1 and NF-κB (Huang CY 2001a; Huang CY 2001b). Previous work in our laboratory demonstrated the hydrogen peroxide can induce MMP9 expression and activity through a MAPK/AP-1 signaling pathway in rat astrocytes (Malcomson E 2011).

Many studies demonstrated the effect of targeting ROS on MMP9. Overexpression of the antioxidant enzyme, superoxide dismutase-1 (SOD1), results in decreased MMP9 expression (Kim GW et al 2003; Morita-Fujimura Y et al 2000). Another study demonstrated that SOD1 protects against spontaneous intracerebral hemorrhage (ICH) in hypertensive mice by reducing the levels of superoxide (Wakisaka Y et al. 2010). These results suggest that ROS and oxidative stress help to mediate the disruption of the BBB by stimulating MMPs.

In cerebral ischemia and traumatic brain injury, hemorrhage occurs and heme/iron is accumulated and deposited in the injury site. Deposition of heme/iron will generate ROS (Abraham NG and Kappas A 2005) and results in the uptake of hemoglobin and heme by surrounding cells, astrocytes and neurons, which is known to be toxic (Matz PG et al. 1997). The uptake of heme occurs through the binding of heme by the blood glycoprotein hemopexin (Aronowski J and Zhao X. 2011). The heme-hemopexin complex is then endocytosed by binding CD91, also known as low-density lipoprotein receptor-related protein-1 (LRP-1). Once internalized, heme is broken down into biliverdin, carbon monoxide (CO), and iron (Aronowski J and Zhao X. 2011). In astrocytes heme uptake occurs by its binding to heme carrier protein 1 (HCP1) which

consequently makes them more susceptible to increased levels of heme (Dang TN et al. 2010; Lara FA et al. 2009).

Heme is known to be a pro-oxidant and is potentially harmful after stroke (Jeney V et al 2002). Both ROS and heme evoke an inflammatory response (Juurlink BH and Sweeney MI 1997; Wagener FA et al. 2001). ROS may also stimulate TNF-α expression in brain cells. The role of heme and iron in producing ROS and evoking inflammation makes it a possible trigger for BBB disruption and increased MMP-9 expression after ischemic stroke. Katsu and colleagues demonstrated that hemoglobin-induced oxidative stress increased MMP9 activity resulting in BBB dysfunction and cell death (Katsu M et al. 2010). They also showed that SOD1 overexpression decreased MMP9 activity following hemoglobin injections and protected against cell death (Katsu M et al. 2010). These results provide further evidence of the important role ROS and oxidative stress play in regulating MMP9 and mediating BBB dysfunction.

1.5 NRF2 and Heme Oxygenase-1

Contrary to the signaling pathways involved in potentiating inflammation and the expression of MMP9, it has been identified that the transcription factor Nrf2 [Nuclear factor (erythroid-derived 2)-like 2] is also activated by ROS and oxidative stress. Nrf2 activation has been identified as a potentially neuroprotective response, responsible for the transcription of many detoxification and antioxidant enzymes such as heme

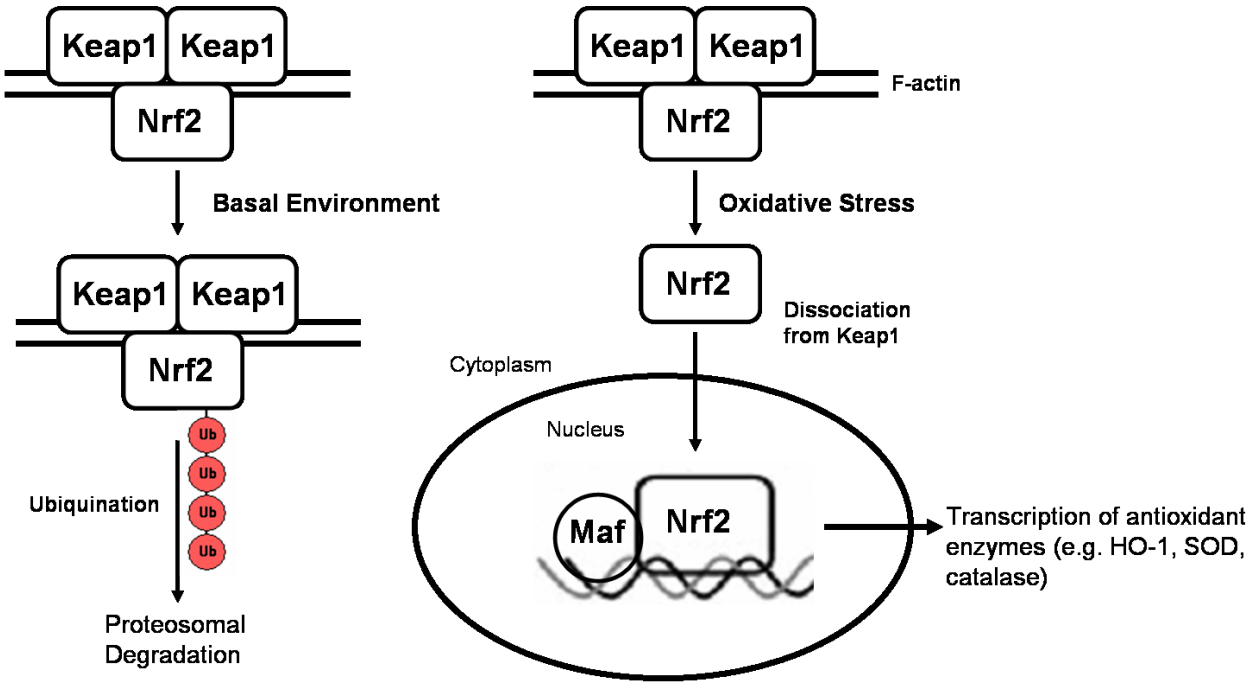

Figure 3. Activation of Nrf2.

Nrf2 is bound to actin by Keap1 in the cytosol under basal conditions. Under conditions of oxidative stress, Keap1 is oxidized changing its structure, which allows the release of Nrf2 and translocation to the nucleus. Once in the nucleus Nrf2 complexes with the small Maf protein and binds the antioxidant response element where it is responsible for the expression of many antioxidant enzymes, such as HO-1.

oxygenase-1 (HO-1), superoxide dismutase, catalase, and glutathione peroxidase (Kensler TW et al. 2007). Under normal conditions Nrf2 is sequestered by Kelch-like ECH-associated protein 1 (Keap1) in the cytoplasm, but under conditions of oxidative stress Keap1 is oxidized allowing for the release of Nrf2 and its translocation to the nucleus where it becomes transcriptionally active (Figure 3) (Negi G et al. 2011). It has been shown that the knockdown of Nrf2 in mice caused severe neurological deficits when subjected to intracerebral hemorrhage (ICH). Additionally, the increased activation of Nrf2 resulted in reduced oxidative damage in ICH brains (Aronowski J and Zhoa X. 2011). Zhoa and colleagues demonstrated that the activation of Nrf2 by sulforaphane increased the expression of protective enzymes in brain tissue and microvessels and resulted in protection against brain injury (Zhoa J et al. 2007). Another study showed that the knockout of Nrf2 resulted in increased activation of NF-κB, and MMP9 expression following spinal cord injury (Mao L et al. 2010). Lastly, an *in vitro* study demonstrated that Nrf2 knockout resulted in increased NF-κB activation, neuroinflammation, and MMP9 expression and activity in primary mouse astrocytes treated with oxyhemoglobin (Pan H et al. 2011). These studies provide the evidence for the potential role of Nrf2 in protecting the brain following cerebral ischemia and oxidative stress.

Heme oxygenase-1 is up-regulated by Nrf2 activation and is the rate-limiting enzyme involved in the breakdown of heme, converting heme to biliverdin, CO, and Fe^{2+} following heme's internalization into the cell (Wang J and Doré S 2007; Wang J and Doré S 2008). Both biliverdin and CO are known anti-oxidant molecules. Chen-

Roetling and colleagues showed that the knockdown of HO-1 in mouse astrocytes resulted in more oxidative injury and cell death (Chen- Roetling J et al. 2005). Conversely, another study demonstrated that the overexpression of HO-1 is cytoprotective (Benvenisti-Zarom L and Regan RF. 2007). Increased HO-1 expression has also been shown to protect astrocytes from hemin, the oxidized for of heme (Benvenisti-Zarom L and Regan RF 2007**;** Chen J and Regan RF 2005; Teng ZP et al. 2004). Paradoxically, inhibition of heme oxygenase activity protects neurons from hemin toxicity (Wang J and Doré S 2007; Koeppen AH et al. 2004).

The goal of this project is to study how heme/iron stimulates MMP9 expression in astrocytes in order to further understand the pathways and mechanisms involved in MMP9 upregulation. Since heme/iron deposits in the brain after cerebral ischemia it may have a role in generating ROS, up-regulating MMP9 expression and thus in the pathogenesis of BBB disruption, leading to secondary brain damage. Understanding how it does so may help to identify new therapeutic targets for relieving BBB disruption in cerebral ischemia and stroke and for treatment of these conditions. This project will focus on characterizing the signaling pathways involved in MMP9 expression stimulated by heme and iron, specifically looking at how heme and iron affects NF-κB and AP-1 mediated MMP9 upregulation.

1.6 Hypothesis and Objectives

1.6.1 Hypothesis

Heme and iron deposited on brain cells will generate ROS and up-regulate the expression of MMP9 in astrocytes via the AP-1 and NFκB signaling pathways.

1.6.2 Objectives

1. Investigate whether heme and iron affect the expression of MMP9 in rat astrocytes.
2. Investigate whether the expression of MMP9 from treatment with heme and iron occurs through the activation of NF-κB and/or AP-1 signaling pathways.
3. Validate whether deposition of heme and iron on cells will generate ROS.
4. Demonstrate that the inhibition of NF-kB or AP-1 signaling pathway affects MMP9 gene expression.

CHAPTER 2: MATERIALS AND METHODS

2.1 Chemical and biochemical reagents

Dulbecco's modified Eagle's medium (DMEM), Antibiotic/Antimycotic, trypsin, Trizol reagent, ultraPure distilled RNase- and DNase-free water, and recombinant rat TNFα were purchased from Invitrogen (Burlington, ON). Hank's balanced salt solution (HBSS) was purchased from Wisent (Montreal, Quebec). Fetal bovine serum (FBS) was purchased from Hyclone (Logan, UT). Dimethyl sulfoxide (DMSO), hemin chloride, iron (II) sulphate, Triton X-100 and were purchased from Sigma (Oakville, ON). Anti-MMP9 Catalytic Domain mAb was purchased from Millipore (Temecula, CA). Monoclonal β-actin perosidase antibody was purchased from Sigma (Oakville, ON). Anti-NFκB (C-20), Anti-Nrf2 (C-20) polyclonal antibodies, and Goat-Anti-Rabbit-IgG Secondary Antibody were purchased from Santa Cruz Biotechnology (Santa Cruz, CA). Anti-C-Jun (60A8) mAb was purchased from Cell Signaling. Anti-rabbit secondary antibody conjugated with Alexa 568 was purchased from Molecular Probes/Invitrogen (Burlington, ON). iScript™ cDNA Synthesis Kit, SsoFast™ EvaGreen® Supermix, PVDF Membrane and BioRad DC Protein Assay kit were purchased from Bio-Rad (Mississauga, ON). Western-Lighting Plus-ECL was purchased from Perkin Elmer Inc. (Waltham, MA). Autoradiography film was purchased from Mandel Scientific (Guelph, Ontario). Ambion DNA-free™ Kit was purchased from Applied Biosystems Inc. (Carlsbad, CA). Nuclear extraction kit was purchased from Affymetrix, Inc. (Santa Clara, CA). LightShift Chemiluminescent EMSA Kit, Chemiluminescent Nucleic Acid Detection Module, DNA 3' End Biotinylation Kit, and Biodyne Nylon Membranes were purchased from Fisher

Scientific (Nepean, Ontario). SP600125, an inhibitor of Jun N-terminal kinase (JNK) was purchased from LC Laboratories (Woburn, MA) and BAY-11-7082, an inhibitor of NFκB, were purchased from EMD Millipore (Billerica, MA).

2.2 Cell Culture

Neonatal rat astrocytes (NRA) were generated from the cortex of 4-8 day old neonatal Sprague-Dawley rats and immortalized with SV40 large T antigen. The immortalized NRA cells were provided by Dr. D. Stanimirovic from the National Research Council of Canada. Passage numbers 80 to 86 were used for the experiments of this study. The cells were maintained in DMEM with the addition of 10% FBS and 1% antibiotic/antimycotic. The medium was changed every second day and cells were plated at an appropriate density depending on the experimental scale. NRA cells were treated with 40 μM hemin chloride, 50 μM iron(II) sulphate, 40 ng/mL recombinant rat TNF-α, and 7.6 mM NaOH (as vehicle). For inhibitor studies NRAs were treated with 15 μM SP600125, and 15 μM BAY-11-7082 along with their vehicle DMSO. Treatments were made up in stale medium.

2.3 RNA isolation, RT-PCR, and Real-time quantitative PCR

2.3.1 RNA isolation

Total RNA was isolated from cultured cells using TRIzol reagent following the manufacturer's instructions. The lysates were transferred to 1.5-mL tubes where chloroform was added. The samples were mixed and then allowed to settle for 2 minutes. Samples were then centrifuged at 14, 000 rpm (18, 000 g) for 15 min at 4^{o}C. Clear

supernatants were collected and transferred to 1.5-mL tubes. Isopropanol was then added to the supernatant and the RNA was left to precipitate (minimum 1 hour to overnight) at 4°C. Following precipitation the samples were warmed to room temperature and were then centrifuged at 10, 000g for 10 min at 4°C. The precipitated RNA pellet was washed one time with 70% ethanol in ultraPure DNase-and RNase-free H_2O. RNA pellets were resuspended in ultraPure DNase-and RNase-free H_2O and heated to 55°C for 10 min. RNA concentration were read at 260 OD values for each sample using NanoDrop 1000 UV-Vis Spectrophotometer (Thermo Scientific Inc., Nepean, ON).

RNA cleanup was performed using DNA-free™ cleanup kit from Invitrogen to remove any genomic DNA following the manufacturer's instructions. RNA samples were incubated with rDNAse I for 30 min at 37°C. Following incubation the DNAse inactivation reagent provided was added and the samples were lightly mixed and left to sit at room temperature for 2 minutes, agitating them every 30 sec. The samples were then centrifuged for 1.5 min at 10,000 rpm to precipitate the stop solution and DNAse. The supernatant was then collected and the concentration was re-determined using NanoDrop 1000 UV-Vis Spectrophotometer (Thermo Scientific Inc., Nepean, ON).

2.3.2 RT-PCR

Reverse transcriptase reaction was performed using 2 µg RNA that was pre-heated with 1 µg Oligo (dT) primers at 70°C for 10 min. After cooling on ice, 5x first strand buffer, 10 mM dNTP, 0.1 M DTT and 50 units of MLV reverse transcriptase were added to the reaction mix and incubated at 42°C for 2 h according to manufacturer's

instructions. For a negative control, RT reaction was performed on a chosen sample as described above with the replacement of the MLV reverse transcriptase with RNAse/DNAse free water. Specific DNA sequences were amplified using PCR master reaction mixture composed of 10 x PCR buffer, 10 mM dNTP, 1.5 mM $MgCl_2$, 10 μM primers, 1.25 units/reaction Taq polymerase, cDNA, and RNase/DNase-free water. PCR primers (Table 1) were synthesized by Alpha DNA (Montreal, Quebec). Six-time loading buffer was added to amplified products and samples were loaded (20 μL/lane for MMP9 and 15 μL/lane for ß-actin) on 1.5 % agarose gel in 0.5 x TBE buffer both containing 0.5 μg/mL ethidium bromide. PCR products were resolved on 1.5% agarose gel by electrophoresis at 100V for approximately 1 hour. The gels were exposed using UV light on Alpha Innotech FluorchemQ system (Santa Clara, California). DNA bands for β-actin and MMP9 from RT-PCR reactions were quantified using densitometry analysis software AlphaVIEW (Cell Bioscience Inc). Final values used to plot bars on graph were determined by taking numerical value of MMP-9 normalized to the corresponding β-actin and comparing fold changes of stimulus vs. vehicle treated cells.

TABLE 1. RT-PCR Primers

Gene	**Primer Sequences**	
MMP9	Forward	5'- AAG GAT GGT CTA CTG GCA C -3'
	Reverse	5'- AGA GAT TCT CAC TGG GGC -3'
β-actin	Forward	5'- GGC TAC AGC TTC ACC ACC AC -3'
	Reverse	5'- TAC TTC CGC TCA GGA GGA GC -3'

2.3.3 RT-qPCR

For reverse transcription reaction the iScript™ cDNA Synthesis Kit from Bio-Rad was used. One microgram (1µg) of RNA was used per reaction. The reaction mixture consisted of the provided 5X iScript reaction buffer, nuclease free water, and the iScript reverse transcriptase. The final reaction volume was 20 µL. The reaction conditions were carried out according to the manufacturer's instructions.

For q-PCR reaction, cDNA was diluted to the appropriate concentration depending on the gene of interest as determined by running standard curves for each gene. The dilutions were 1/4 for MMP9 and 1/100 for GAPDH and HO-1. GAPDH was used as the reference gene as determined by using the reference gene assay kit from Primer Design following the manufacturer's instructions. In brief, the set of primers provided were all run on the treated sample from the NRA cells. The data was then analyzed using the GeNorm software which identified the most stable reference gene under the treatment conditions. qPCR reactions were carried out using the SsoFast™ EvaGreen® Supermix from Bio-Rad. Each reaction consisted of 2µL cDNA, 10µL of the SsoFast™ EvaGreen® Supermix, 6µL of ultraPure DNase-and RNase-free H_2O, and 1µL each of the forward and reverse primers. Primers were synthesized by Integrated DNA technologies (IDT) and are listed in Table 2. qPCR reactions were carried out using the CFX96^{TM} Real Time System C1000^{TM} Thermocycler from Bio-Rad.

TABLE 2. Real Time Quantitative PCR Primers

Gene	Primer Sequences	
MMP9	Forward	5'- TGG TTA TCG CTG GTG CGC CAC -3'
	Reverse	5'- CAG TGA CGT CGG CTC GAG TAG G -3'
HO-1	Forward	5'- CAC TGG CAT GGC CTT CCG TGT T -3'
	Reverse	5'- TAC TTG GCA GGT TTC TCC AGG CGC -3'
GAPDH	Forward	5'- GGC CTG CTA GCC TGG TTC AAG ATA C -3'
	Reverse	5'- AAT TCC CAC TGC CAC GGT CGC -3'

2.4 ROS Assay

NRA cells were plated and grown in 96-well culture plates to approximately 90% confluency. Medium was aspirated from the cells and the ROS probe (2',7'-dichlorodihydrofluorescein diacetate; H_2DCFDA) was added at a concentration of 10 μM in clear HBSS. Cells were incubated for 30 min at 37^{o}C and 5% CO_2 for 30 min. Following incubation with the probe the cells were washed with clear HBSS and treatments were added. The cells were treated with 40 μM hemin chloride, 50 μM iron(II) sulphate, and 7.6 mM NaOH (as vehicle) diluted in base DME media (serum free). Immediately following the addition of the treatment the plate was read with the Fluoroskan Ascent plate reader to assess fluorescence using excitation 492 and 540 nm emission filters. Readings were taken every 30 min for 2 hours. Following the reading of the plate the plate was stored at -20^{o}C overnight and Hoechst staining was performed the following day. Hoechst stain was added at a 1:10 000 dilutions for 30 min. The plate

was read using the Fluoroskan Ascent plate reader using excitation 355 and 460 nm emission filters.

2.5 Electrophoretic Mobility Shift Assay (EMSA)

NRA cells were grown in 60-mm culture dishes. When reached approximately 90% confluency the cells were treated with 40 μM hemin chloride, 50 μM iron(II) sulphate, 40 ng/mL recombinant rat TNF-α, and 7.6 mM NaOH (as vehicle). For inhibitor studies NRAs were treated with 15 μM SP600125, and 15 μM BAY-11-7082 along with their vehicle DMSO. Treatments were made up using stale media. Following treatment nuclear isolations were performed using the nuclear extraction kit from Panomics Inc following manufacturer's instruction. Cells were washed with ice cold PBS. Following washing Buffer A containing the provided protease inhibitors and DTT was added and the dishes were shaken on ice for 10 min. Afterwards the lysates were transferred to 1.5 mL tubes and centrifuged for 3 min at 14, 000 rpm at 4^{o}C. The supernatant was removed and Buffer B containing the provided protease inhibitors and DTT was added. The samples were left to sit on ice for 1 hour with gentle mixing every 20 min. Samples were then centrifuged for 5 min at 14, 000 rpm at 4^{o}C and the supernatant was transferred to a new 1.5 mL tubes. The quantification of the protein concentration from the nuclear extracts was done using the Bio-Rad DC Protein Assay kit.

Oligonucleotide probes were purchased from IDT and 3' End Biotin labeled using the 3' End Biotinylation Kit from Fisher Scientific (Table 3) following manufacturer's

instructions. Probes were labeled in a reaction mixture consisting of DNase-and RNase-free H_2O, Terminal deoxynucleotidyl transferase (TdT) reaction buffer, Biotin-11-UTP, and TdT. Reactions were incubated at 37^{o}C for 30 min. EDTA (0.2 M, pH 8.0) was then added to stop the reaction. The labelled probes were then extracted from the reaction mixture by the addition of chloroform: isoamyl alcohol (24:1). The mixtures were mixed and then centrifuged for 1-2 min at high speed. The top phase containing the labelled probes was transferred to a new tube. Complementary probes were then annealed by adding equal volumes of each probe. The probes were then heated to 90^{o}C for 1 min and then allowed to slowly cool to room temperature.

EMSAs were performed using the LightShift Chemiluminescent EMSA Kit from Fisher Scientific. EMSA binding reactions were carried out using 5µg of nuclear protein extract. The reaction was carried out in the provided binding buffer, along with DNase- and RNase-free H_2O, poly dI-dC, glycerol, $MgCl_2$, EDTA, and biotin-end labelled probes. The final reaction volume was 20 µL. For reactions receiving antibodies the mixture was incubated for 5 min with the antibody at room temperature prior to the addition of the probe. Following the addition of the probe the reactions were left at room temperature for 20 min to allow binding. EMSA loading buffer was added to each reaction. Reactions were separated using a 5% acrylamide gel prepared in 0.5X TBE that was pre-run for 30 min at 100V in 0.5X TBE. The binding reactions were then transferred to biodyne nylon membranes in an electrophoretic transfer unit with cooled 0.5X TBE. Transfer was carried out at 1 ampere for approximately 1.5 hour. After

transfer the membranes were UV cross-linked for 15 min on a transilluminator equipped with a 312nm bulb.

Membranes were developed using the chemiluminescent nucleic acid detection module from Fisher Scientific. Membranes were blocked for 15 min in 20 mL of the provided blocking solution that was warmed to 37^{o}C. The membranes were then incubated in streptividin-HRP secondary at a 1:300 dilution in blocking buffer. Membranes were then rinsed with 20 mL of pre-warmed washing buffer as provided by the kit, and then washed 4 times with 20 mL of the washing buffer for 5 min. Following the washes, membranes were placed in 30 mL of the provided substrate equilibration buffer for 5 min. Membranes were then placed face down on 8 ml of 1:1 mixed luminol/enhancer and stable peroxide solution for 5 min. Membranes were visualized using X-ray films.

TABLE 3. EMSA Oligonucleotide Probes

Transcription Factor	**Oligonucleotide Sequences**	
AP-1	Forward	5'- CGC AAG TGA CTC AGC GCG -3'
	Reverse	5'- CGC GCT GAG TCA CTT GCG -3'
NFκB	Forward	5'- TTT CGC GGG GAC TTT CCC GCG C -3'
	Reverse	5'- TTT GCG CGG GAA AGT CCC CGC G -3'
Nrf2	Forward	5'- CGG TCA CCG TTA CTC AGC ACT TTG -3'
	Reverse	5'- CAA AGT GCT GAG TAA CGG TGA CCG -3'

2.6 Western Blot

NRA cells were grown in 12-well culture plates and were treated with 40 μM hemin chloride and 50 μM iron (II) sulphate for 2 and 8 hours. Following treatment cells were washed 2 times in colour-free HBSS and then lysed in loading buffer. Lysates were shaken for 10 min and then transferred to 1.5-mL tubes. Lysates were then vortexed and put on ice for 3 min, boiled for 10 min at 100^{o}C, cooled on ice for 5 min and then centrifuged at 14,000 rpm for 10 min at 4˚C. Supernatant was transferred to new 1.5-mL tubes. Protein concentration was determined using trichloroacetic acid (TCA) protein assay. TCA assay was done on a 96-well plate with a bovine serum almunin (BSA) standard curve in order to determine protein concentrations, from 30 μL of each sample done in duplicate. TCA was added to initiate the reaction, and the plate was incubated for 15 min at 37^{o}C and then read by a Spectra MAX 340 spectrophotometer under 570 nm (Molecular Devices Inc.) using SoftMax PRO program. Equal amounts (μg) of protein were loaded on 10% SDS-PAGE gels. Proteins were transferred to PVDF membrane at 150 mA overnight. Blots were blocked for 1 hour at room temperature in fresh blocking buffer [0.1 % Tween-20 in Tris-buffered saline (TBST), pH 8.0, containing 5% non-fat dried milk). Primary antibody for Anti-MMP-9 Catalytic Domain mAb (Millipore) was made up at a dilution of 1:1000 in 0.1% TBST containing 1% non-fat dried milk and the blots were incubated overnight at 4◦C. The blots were washed 5 times in 0.1% TBST, then were incubated with 1:5000 dilution of secondary antibody conjugated with horseradish peroxidase (donkey anti-rabbit IgG) (Santa Cruz Inc) in 0.1% TBST containing 5% non-fat dried milk for 1 h at room temperature. Blots were washed again

3 times with 0.1% TBST and were developed using ECL Plus substrate solution for 5 min according to manufacturer's instructions and visualized using X-ray film.

2.7 Immuncytochemistry

NRA cells were plated in 12-well culture plates in which each well contained a 12-mm glass coverslip until they reached 75% confluency. The cells were the then treated with 40 μM hemin chloride, 50 μM iron(II) sulphate, 40ng/mL recombinant rat TNF-α, and 7.6 mM NaOH (as vehicle). Following treatment cells were washed 1 time with clear HBSS and then fixed using ice cold methanol for 5 min. Cells were then washed 4 times with HBSS and then made permeable using 0.1% Triton-X-100 for 10 min at room temperature. Cells were washed 3 times for 5 min each with HBSS. Cells were then blocked overnight at 4^{o}C using 4% normal goat serum in HBSS. Primary MMP9 antibody was then added at 1/100 dilution in 1% goat serum. For secondary alone, 1% goat serum in HBSS was added. Cells were then washed 2 times for 5 min each in HBSS and secondary was then added. Alexa568-conjugated anti-rabbit antibody at a 1:500 dilution in HBSS was added to the cells for 30 min at room temperature in the dark. Cells were washed 3 times in HBSS for 5 min and Hoechst 33342 at a 1:5000 dilution in HBSS was added for 15 min. Images were taken with the Olympus FV1000 confocal microscope at 20 and 40 times magnification.

2.8 Statistical analysis

Data were presented as mean ± SD. Statistical analysis for single comparison was performed by paired or unpaired Student's *t*-test. Statistical analysis for group comparison where a single factor was being analyzed was performed by one-way ANOVA with Bonferroni's post-test. Statistical analysis for group comparison where two factors were analyzed was performed by two-way ANOVA with Bonferroni's post-test. The criteria for significance for all tests was $p<0.05$. All statistical test were performed on experiments carried out at least 3 times (n=3).

CHAPTER 3: RESULTS

3.1 Effect of Heme and Iron on MMP9 Expression in Rat Astrocytes

Following cerebral ischemia or ischemic stroke there can be intracerebral hemorrhage and subsequent bleeding into the brain leading to the deposition of heme and iron. In order to determine whether MMP9 expression is regulated by the deposited heme and iron, NRA cells were treated with various concentrations of the heme analogue, hemin chloride (20, 40, and 100 μM) with or without 50 μM iron (II) sulfate for 2 hours. TNF-α was used as a positive control since it has previously been shown to upregulate MMP9 expression. Total RNA was isolated and RT-PCR was performed. Figure 4 shows that treatment with heme and heme/iron caused an increase in MMP9 gene expression in rat astrocytes with the optimal concentration found to be 40 μM hemin chloride ($p<0.01$ by paired *t*-test). This concentration was used throughout the rest of this study to investigate the mechanisms and regulation of heme-induced MMP9 expression.

3.2 Heme and Iron Increase MMP9 and HO-1 Expression

Following the determination of the effect of heme and heme/iron treatment on MMP9 expression in the rat astrocytes, a time-course looking at MMP9 expression was performed. NRA cells were treated with heme and iron as previously described. Total RNA samples were collected and RT-qPCR was performed to look at MMP9 gene expression. Figure 5A shows the effect of heme and iron treatment on MMP9 expression. Heme and heme/iron treated cells showed a significant increase in MMP9 gene expression at 2 hours. A fold increase of 2.01±0.471 ($p<0.01$ by unpaired *t*-test, N=3)

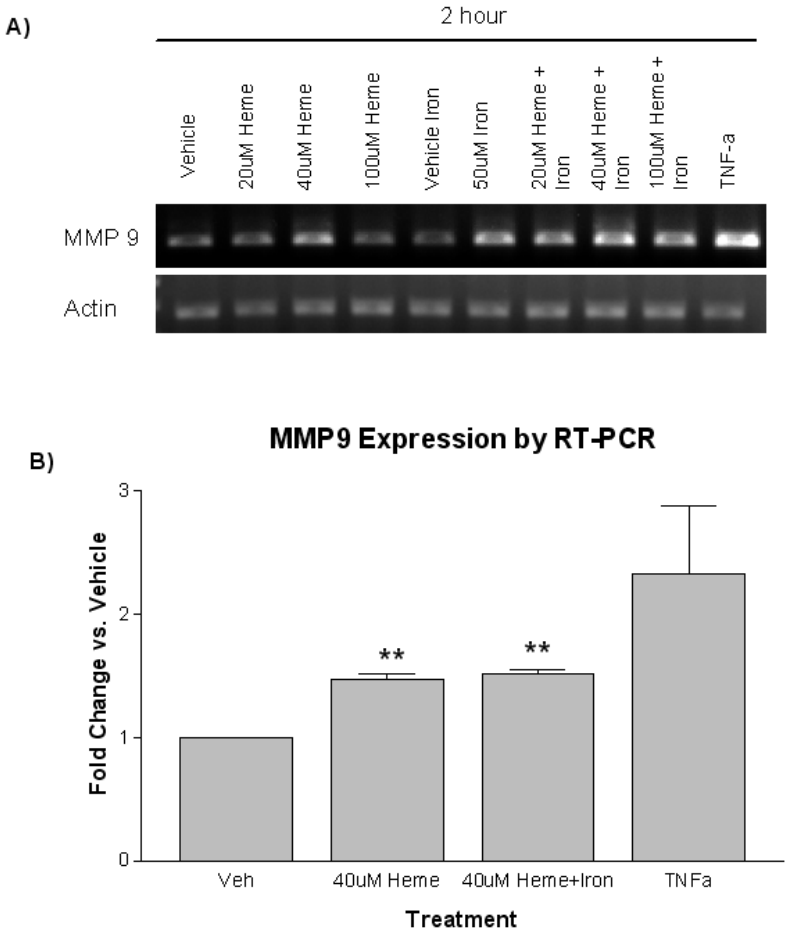

Figure 4: Effect of Heme and Iron on MMP9 Expression. NRA cells were treated with various concentrations of hemin chloride (20, 40, and 100 μM) and in combination with 50 μM iron (II) sulphate for 2 hours. Vehicle treatment for hemi chloride was 7.6 mM NaOH and Vehicle for iron was ultrapure water. RNA was isolated and RT-PCR was performed. Panel A): Agarose gel representation showing the effects of heme/iron treatment. Treatment with 40 μM hemin chloride was determined to be optimal for induced expression on MMP9. Panel B): Densitometry of 40 μM hemin and hemin with iron at 2 hours. **: $p<0.01$ by paired Student's *t*-test compared to vehicle. (N=3)

A)

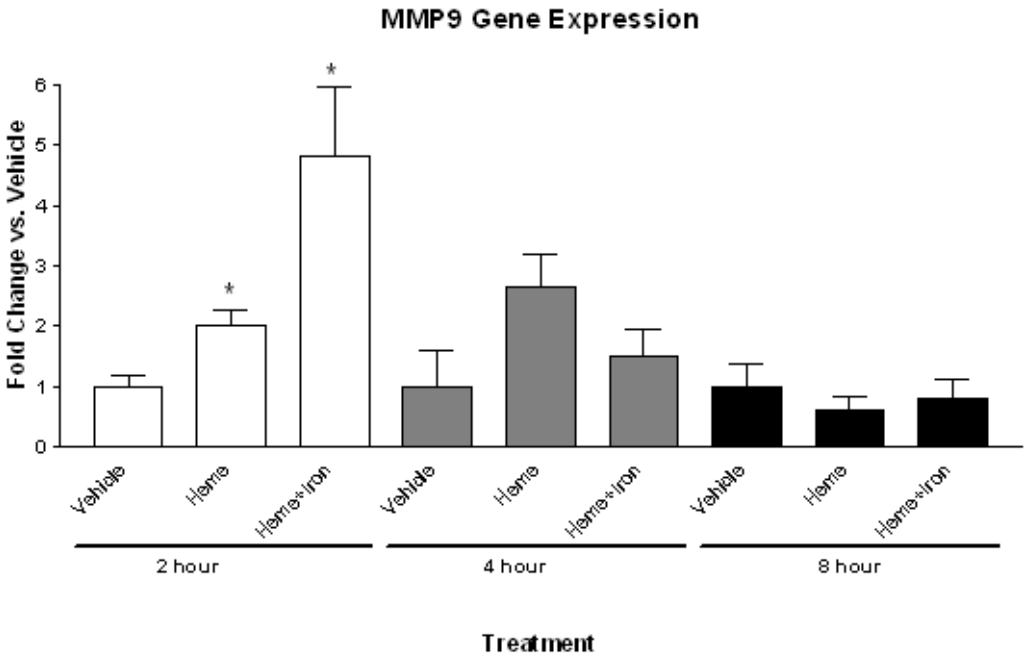
MMP9 Gene Expression
Fold Change vs. Vehicle
0
1
2
3
4
5
6
*
*
Vehicle
Heme
Heme+Iron
Vehicle
Heme
Heme+Iron
Vehicle
Heme
Heme+Iron
2 hour
4 hour
8 hour
Treatment

B)

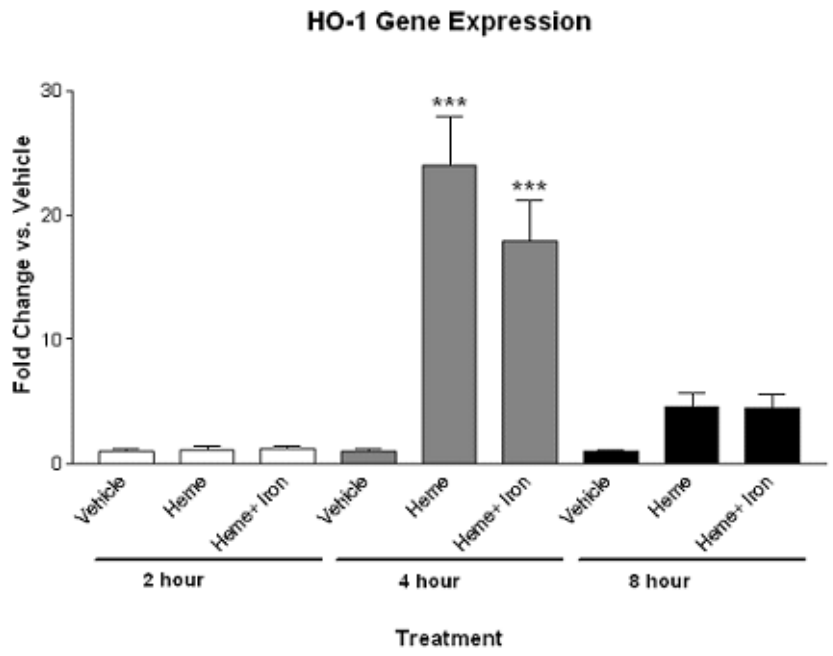
HO-1 Gene Expression
Fold Change vs. Vehicle
0
10
20
30
***
***
Vehicle
Heme
Heme+ Iron
Vehicle
Heme
Heme+ Iron
Vehicle
Heme
Heme+ Iron
2 hour
4 hour
8 hour
Treatment

Figure 5: The Effect of Heme and Iron on MMP9 and HO-1 Expression in Rat Astrocytes. NRA cells were treated for 2, 4 and 8 hours with 40 μM hemin chloride and 50 μM iron (II) sulfate. Vehicle treatment is 7.6 mM NaOH. RNA samples were collected and RT-qPCR was performed. Panel A): Heme and heme/iron treatment induced MMP-9 gene expression at 2 hours and this increased expression was not present at 8 hours. *: $p < 0.05$ by Two-Tailed *t*-test compared to Vehicle B): HO-1 gene expression was increased at 4 hours. One-way Anova (***$p<0.0001$) Bonferroni's post-hoc test ($p <0.001$) (N=3)

was observed at 2 hours for heme treated NRA cells, while a fold increase of 4.83±1.97 ($p<0.01$ by unpaired *t*-test, N=3) was observed for heme/iron treated cells. Figure 5A demonstrates that MMP9 expression was quickly upregulated at 2 hours and that this increased expression remained slightly elevated at 4 hours and returned to control levels by 8 hours.

Since the stimulus being used in the study was heme and iron, the expression of heme oxygenase-1 was also of importance due to its role in the degradation of heme and protection from oxidative stress. Figure 5B shows that heme oxygenase-1 expression was increased by the heme and heme/iron treatment, as expected. HO-1 expression was greatly increased at 4 hours by both treatments. The fold increases of 23.96±6.88 ($p<0.001$ by One-way ANOVA with Bonferroni post-hoc test, N=3) and 17.86±5.76 ($p<0.001$ by Bonferroni post-hoc test, N=3) were observed for heme and heme/iron treated cells, respectively. HO-1 levels remained elevated at 8 hours (Fig. 5B) with the levels being 4.63± 1.89 for heme and 4.44± 1.05 for heme/iron treated NRA cells. The increase in HO-1 expression at 4 hours coincided with decreasing levels of MMP9 indicating a potential protective effect of increased HO-1 against heme induced MMP9 expression.

3.3 Activation of AP-1, NFκB, and Nrf2 signaling pathways by Heme and Iron

To determine the potential pathways involved in upregulating the expression of MMP9 by heme and iron in NRA cells, EMSA was performed to look at AP-1 and NFκB activation. NRA cells were treated as previously described and nuclear isolations were collected. Figure 6A and 6D show that heme and heme/iron treatment for 2 hours caused an increase in AP-1 activation with respective fold increases of 1.68±0.463 ($p<0.05$ by two-tailed *t*-test, N=5) and 1.94±0.896 compared to vehicle treated cells. A control reaction containing a total c-Jun antibody was also performed and caused decreased binding of AP-1 to the oligonucleotide probe, confirming that the band is AP-1 and that the AP-1 heterodimer contains the c-Jun subunit . EMSA for NFκB demonstrated a trend in the transcription factors activation in both the heme and heme/iron treated cells with fold increases of 1.485± 0.458 and 1.524± 0.740 compared to vehicle at 2 hours, but this result was not statistically significant (Figure 6B). Similarly to AP-1, a control was performed using an NFκB antibody. Incubation with the antibody prevented binding to the probe indicating that the obtained band is NFκB.

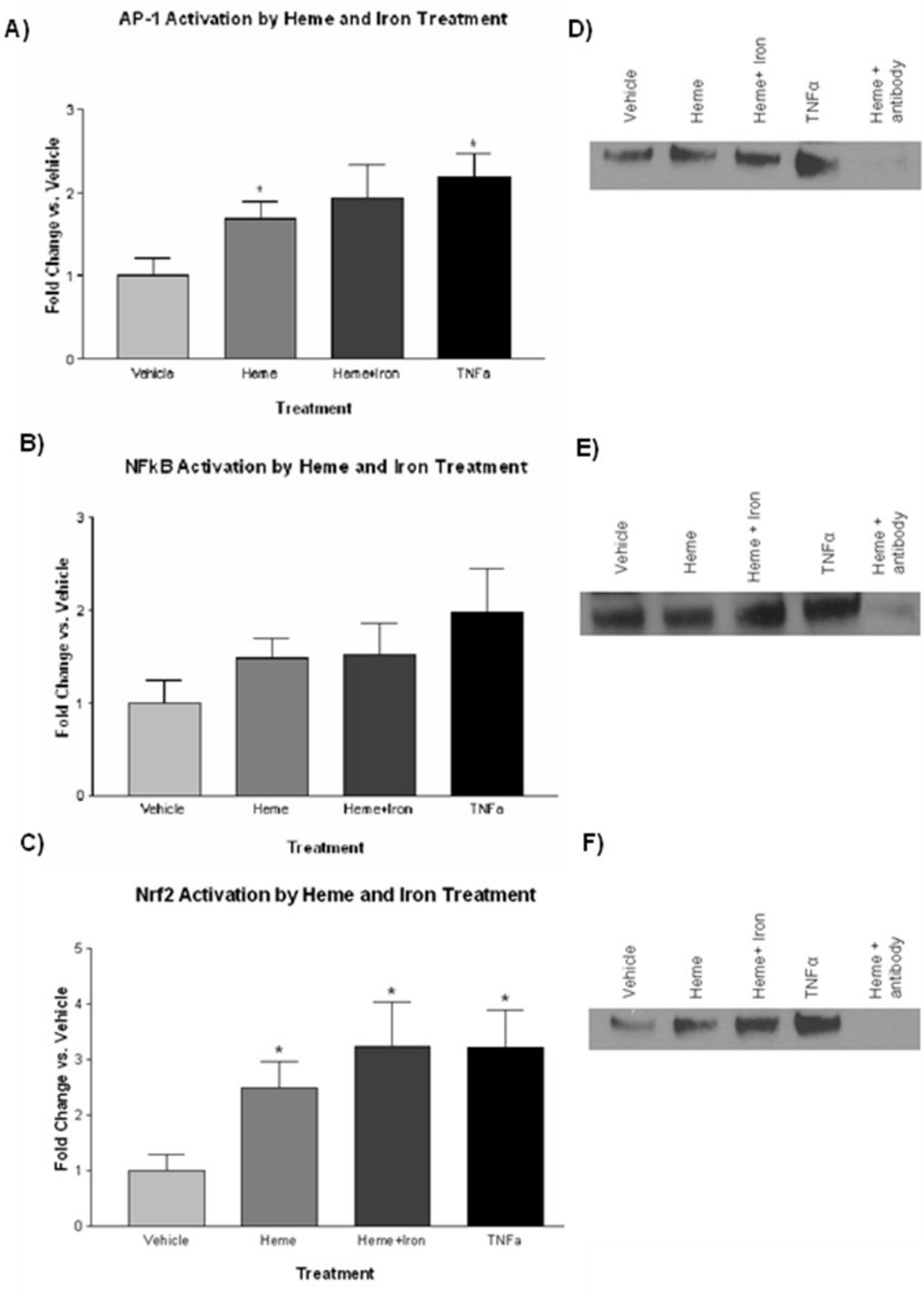
A)
AP-1 Activation by Heme and Iron Treatment
Fold Change vs. Vehicle
Vehicle
Heme
Heme+Iron
TNFa
Treatment
B)
NFkB Activation by Heme and Iron Treatment
Fold Change vs. Vehicle
Vehicle
Heme
Heme+Iron
TNFa
Treatment
C)
Nrf2 Activation by Heme and Iron Treatment
Fold Change vs. Vehicle
Vehicle
Heme
Heme+Iron
TNFa
Treatment
D)
Vehicle
Heme
Heme+ Iron
TNFα
Heme + antibody
E)
Vehicle
Heme
Heme + Iron
TNFα
Heme + antibody
F)
Vehicle
Heme
Heme+ Iron
TNFα
Heme + antibody

Figure 6: EMSA for Activation of AP-1, NFκB and Nrf2 in Rat Astrocytes Treated with Heme and Iron: NRA cells were treated for 2 hours with 40 μM hemin chloride and 50 μM iron (II) sulfate. Vehicle treatment is was 7.6 mM NaOH. EMSA binding reactions were performed using nuclear isolations. Supershift was done using a total c-Jun, an NFκB and an Nrf2 antibody, respectively. Panel A): AP-1 EMSA. Heme treatment shows an increase in AP-1 activation over Vehicle (N=5). Panel B): NFκB EMSA (N=5). Panel C) shows activation of Nrf2 by heme and iron treatment (N=5, * $p < 0.05$ by Two-Tailed *t*-test compared to Vehicle).

Additionally, EMSA to measure the activation of Nrf2, the transcription factor responsible for the expression of HO-1, was performed. Figure 6C and 6F shows that heme and heme/iron treated NRA cells have increased activation of Nrf2 with fold increases of 2.496±1.02 ($p<0.05$ by two-tailed *t*-test, N=5) and 3.22± 1.49 ($p<0.05$ by two-tailed *t*-test, N=5) compared to vehicle at 2 hours. Confirmation of the band was performed using an Nrf2 antibody which prevented binding to the probe. These results identify some potential pathways involved in the expression and regulation of MMP9 following heme and iron deposition in the brain.

3.4 Heme and Iron Generate ROS

It is well known that heme and iron can generate ROS, and that ROS are stimuli for the activation of the AP-1 and NFκB signaling pathways. In order to determine the amount of ROS generated by the heme and iron treatment a ROS assay was performed. Figure 7 shows that there was a significant increase in ROS produced by heme and heme/iron following 2 hours of treatment, with the respective fold increases being 1.90±0.298 ($p<0.01$ by Bonferroni's post-hoc test, N=3) and 1.90±0.153 ($p<0.01$ by Bonferroni's post-hoc test, N=3) compared to vehicle treatment. This suggests that the observed increase in MMP9 mRNA expression and activation of the AP-1 and NFκB signaling pathways may be caused due to the production of ROS by heme and iron treatment.

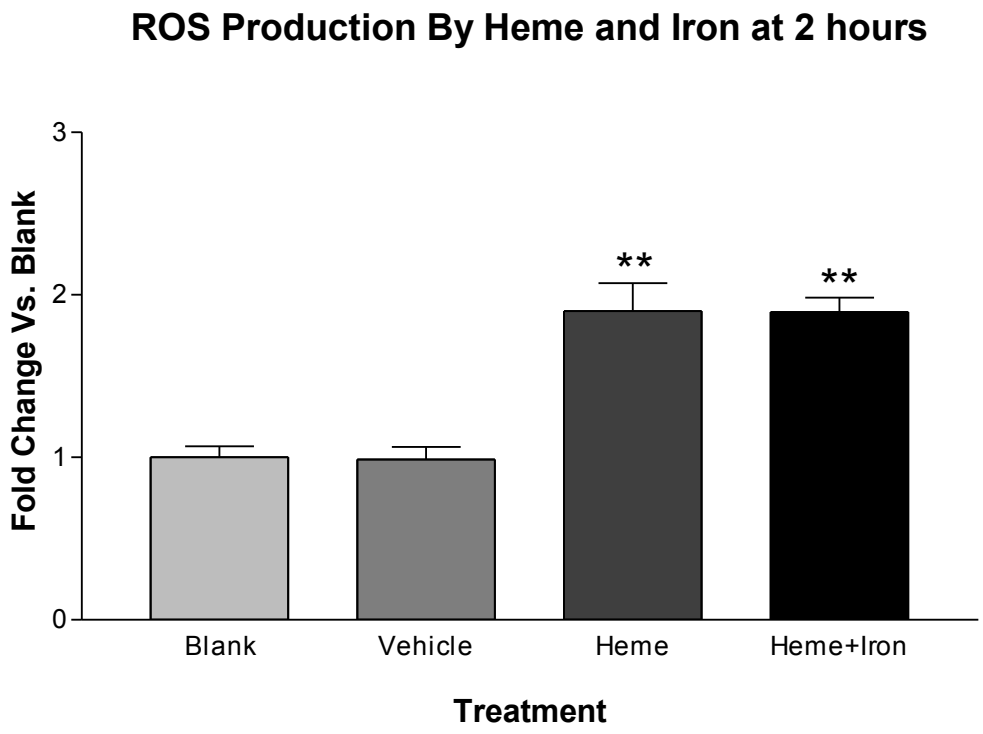

Figure 7: The Production of ROS by Heme and Iron: The generation of ROS produced by heme and iron treatment was determined by ROS assay. NRA cells were treated with 40 μM hemin chloride and 50 μM iron (II) sulfate. Vehicle treatment was 7.6 mM NaOH and blank treatment was basal DME media. ROS assay was performed using the H_2DCFDA substrate. Results were normalized to the blank treatment. It is observed that at 2 hours following treatment there was a significant increase in the production of ROS in both the heme and heme/iron treated cells. One-way Anova: $p=0.0003$ **: $p<0.01$ by Bonferroni's post-hoc test compared to Vehicle (N=3).

3.5 AP-1 and NFκB Inhibition Prevents Increased MMP9 Expression by Heme and Iron

In order to validate that AP-1 and NFκB are responsible for the increase in MMP9 gene expression, cells were treated with SP600125 (JNK inhibitor), MG132 (NFκB inhibitor) and BAY-11-7082 (NFκB inhibitor) and RT-qPCR was performed. SP600125 functions by preventing JNK from phosphorylating c-Jun which activates AP-1. Figure 8A demonstrates that inhibition of JNK resulted in a decrease in MMP9 expression at 2 hours. Treatment with 15μM SP600125 reduced MMP9 expression in heme treated cells from 3.90±1.57 to 2.15±1.23 and in heme/iron treated cells from 5.47±3.01 to 1.38±1.09 ($p<0.05$ by two tailed *t*-test, N=4). This result indicates that AP-1 plays a role in up-regulating the expression of MMP9 following heme and iron treatment.

The role of NFκB was investigated using two inhibitors, MG132 and BAY-11-7082. MG132 inhibits NFκB by stopping proteosomal degredation of IκB-α, the protein that keeps NFκB sequestered in the cytosol and transcriptionally inactive. Treatment with 10 μM MG132 in combination with heme and heme/iron caused a significant decrease in MMP9 expression after 2 hours of treatment. In heme and heme/iron treated cells a decrease of 2.43± 1.50 to 1.50± 0.861 and 4.51± 1.53 to 1.32± 0.254 (One-way ANOVA, $p<0.05$ by Bonferroni's post-hoc test, N=3) was observed, respectively. Since MG132 inhibits the proteosome, it is not a very selective NFκB inhibitor. In order to verify the results, a more selective inhibitor BAY-11-7082 was used. BAY-11-7082 inhibits NFκB by preventing the phosphorylation and activation of IKK, the kinase responsible the phosphrylation of IκB-α and activation of NFκB (Lee et al. 2012).

A)

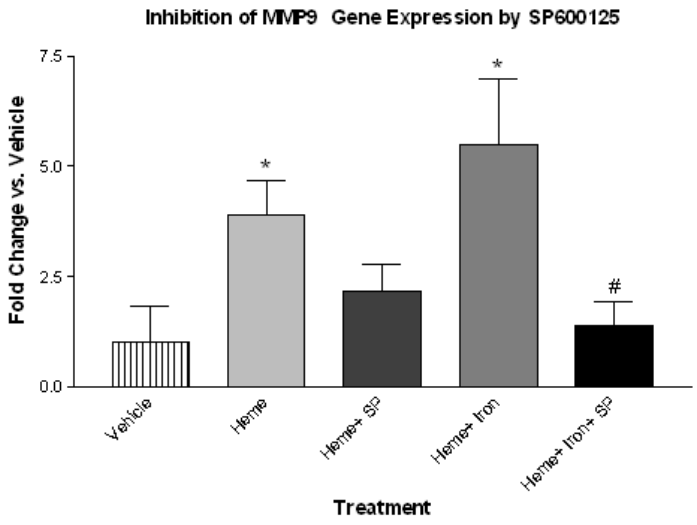
Inhibition of MMP9 Gene Expression by SP600125
Fold Change vs. Vehicle
7.5
5.0
2.5
0.0
*
*
#
Vehicle
Heme
Heme+ SP
Heme+ Iron
Heme+ Iron+ SP
Treatment

B)

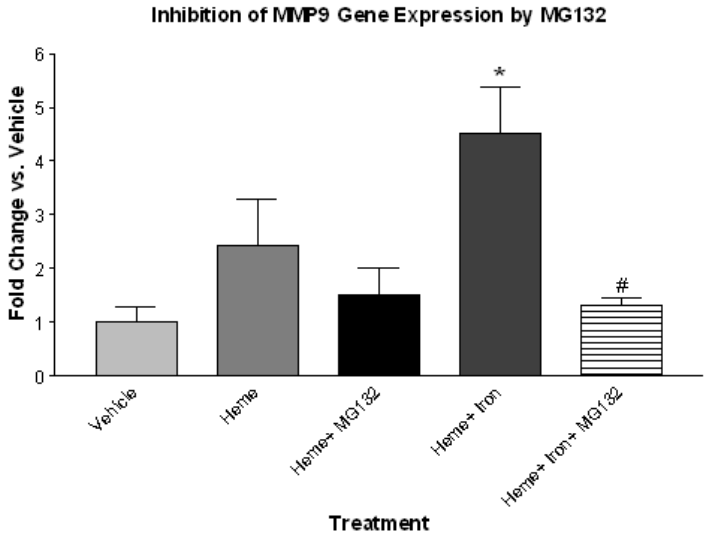
Inhibition of MMP9 Gene Expression by MG132
Fold Change vs. Vehicle
6
5
4
3
2
1
0
*
#
Vehicle
Heme
Heme+ MG132
Heme+ Iron
Heme+ Iron+ MG132
Treatment

C)

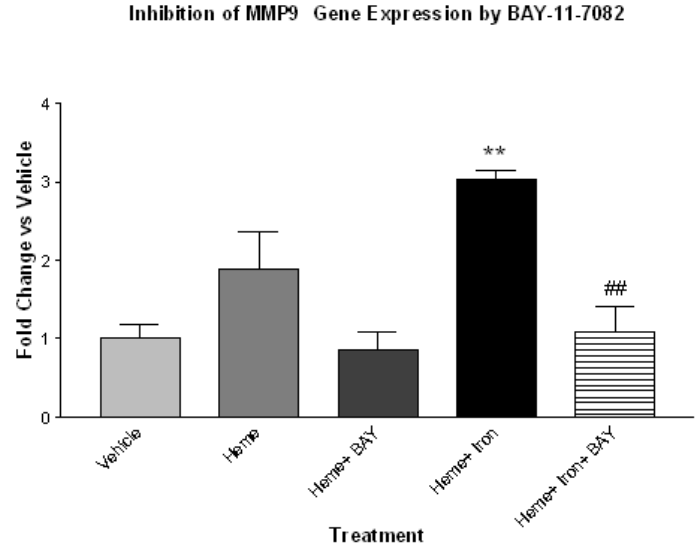
Inhibition of MMP9 Gene Expression by BAY-11-7082
Fold Change vs Vehicle
4
3
2
1
0
**
##
Vehicle
Heme
Heme+ BAY
Heme+ Iron
Heme+ Iron+ BAY
Treatment

Figure 8: RT-qPCR to determine the Effects of JNK-AP1 and NFκB Inhibitors on MMP9 Expression. NRA cells were treated for 2 hours with 40 μM hemin chloride and 50 μM iron (II) sulfate. Panel A): Treatment with 15 μM SP600125 (JNK inhibitor) caused a decrease in MMP9 gene expression in heme and iron treated NRAs (N=4. * $p< 0.05$ by Two-Tailed *t*-test compared to Vehicle. #$p< 0.05$ by Two-Tailed *t*-test compared to heme + iron). Panel B): Treatment with 10 μM BAY-11-7082 (NFκB inhibitor) caused a decrease in MMP9 expression in heme and iron treated cells (N=3, One-way Anova $p=0.0017$ ** $p< 0.01$ by Bonferroni's post-hoc test compared to Vehicle. ##: One-way ANOVA, $p<0.01$ by Bonferroni's post-hoc test compared to heme + iron). Panel C): Treatment with 10 μM MG132 (NFκB inhibitor) caused a decrease in MMP9 expression in heme and iron treated cells (N=3, One-way Anova $p=0.0141$ * $p< 0.05$ by Bonferroni's post-hoc test compared to Vehicle. # $p<0.05$ by Bonferroni's post-hoc test compared to heme + iron).

Treatment with the BAY-11-7082 also caused a significant reduction in the expression of MMP9 at 2 hours following treatment with heme and heme/iron. MMP9 expression was reduced from 1.89±0.805 to 0.851±0.398 in heme treated NRA cells and 3.03±0.214 to 1.09±0.547 ($p<0.01$ by Bonferroni's post-hoc test, N=3) in heme/iron treated cells (Figure 8B). The results using the two NFκB inhibitors were similar indicating that NFκB plays a role in the regulation of the expression of MMP9 and that this signaling pathway can be targeted at multiple locations to achieve inhibition of MMP9 expression. Since MMP9 expression can be up-regulated via both MAPK-AP1 and NFκB signaling pathways, the signals may be summed at the promoter of MMP9. Similarly, the inhibitory signals may be also added at the promoter region of MMP9, leading to reduced expression of MMP9.

EMSA was performed to verify the role of AP-1 in upregulating MMP9 expression. NRA cells were treated with heme and iron in combination with SP600125. Figure 9A shows that treatment with 15 μM SP600125 in combination with heme and heme/iron resulted in a decrease in AP-1 activation at 2 hours. The observed decrease was 1.42± 0.389 to 0.752± 0.859 and 1.79± 0.392 to 0.947± 0.465 in heme and heme/iron treatments. This provides further evidence that the decrease in MMP9 expression observed in Figure 8A by SP600125 was occurring through the inhibition of AP-1. To confirm that NFκB may also be responsible for the upregulation of MMP9, cells were treated using the NFκB inhibitor, BAY-11-7082, for 2 hours. Figure 9B shows that treatment with 15μM BAY resulted in a slight decrease in NFκB activation, 1.43± 0.057 to 1.06± 0.121 for heme and 1.26± 0.176 to 0.800± 0.365 for heme/iron. This result also

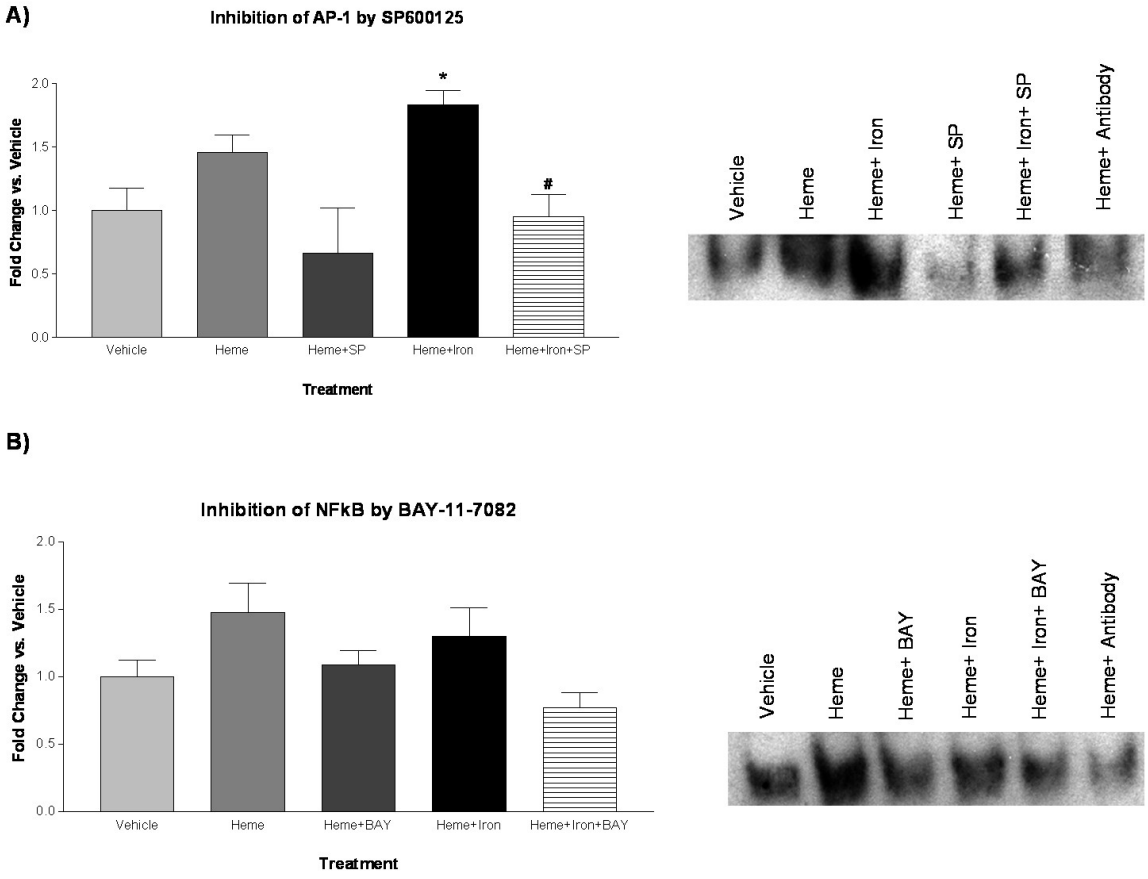

Figure 9: The Effects of JNK-AP1 and NFκB Inhibitors on the Activation of the Transcription Factors. NRA cells were treated for 2 hours with 40 μM hemin chloride and 50 μM iron (II) sulfate. Vehicle treatment is 7.6mM NaOH. EMSA binding reactions were performed using nuclear isolations. Supershift was done using a total c-Jun and NFκB antibody. Panel A): Treatment with 15 μM SP600125 (JNK inhibitor) caused a decrease in AP-1 activation in the heme and heme+ iron treated NRAs (N=3). Panel B): Treatment with 10 μM BAY-11-7082 (NFκB inhibitor) caused a decrease in NFκB activation in the heme and heme+ iron treated NRAs (N=3).

provides further evidence that NFκB may play a role in MMP9 upregulation following heme and heme/iron treatment.

3.6 MMP9 Protein Expression

Western blot was performed to look at the protein expression of MMP9 in heme and iron treated NRA cells. Figure 10 shows that after 2 hours of treatment that there is no change in the overall levels off pro-MMP9 (Figure 10A and 10B). No active MMP9 was detected on the western blots (Figure 10A) indicating that even though heme and iron treatment had increased MMP9 gene expression at the mRNA level, it had not increased pro-MMP9 and active MMP9 in the experimental model.

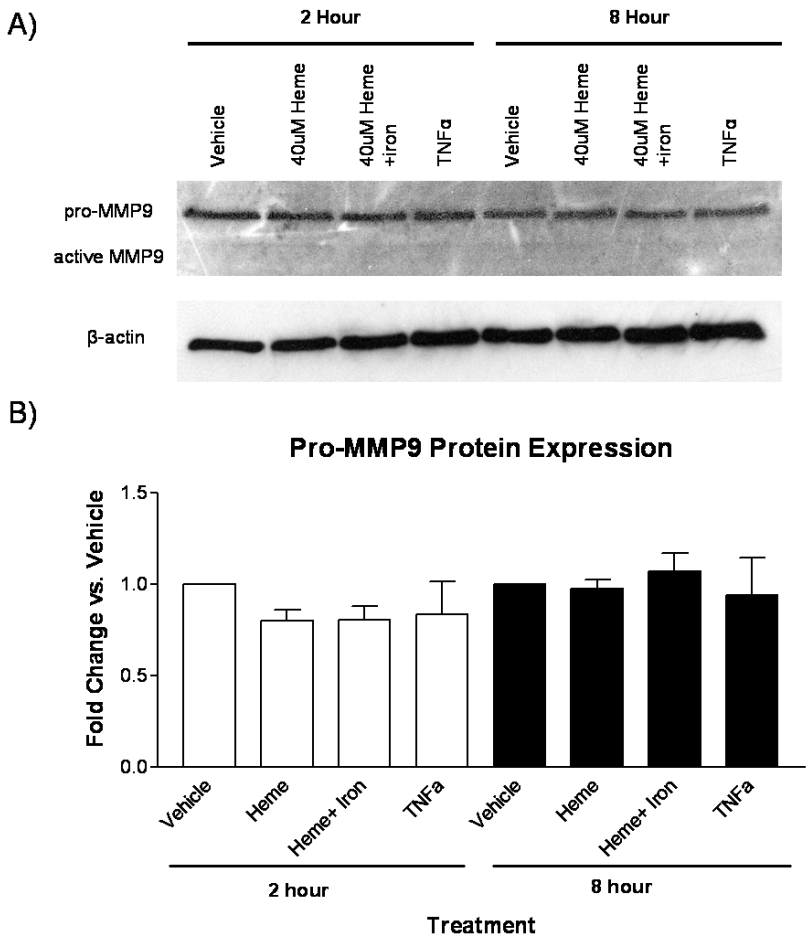

Figure 10: Western Blot Detection of pro-MMP9 in Treated NRA cells

Western blot for NRA cells treated with 40 μM hemin chloride and 50 μM iron (II) sulfate for 2 and 8 hours. Panel A shows a representative Western blot for pro-MMP9 (92kDA) and β-actin. Panel B is the densitometry analysis. (N=3)

3.7 Detection of MMP9 Protein by Immunocytochemistry

In order to observe whether the increase in MMP9 gene expression observed in heme and iron treated NRAs was also present at the protein level immunofluorescent detection for MMP9 was performed. Figure 11 shows merged images of the cell nuclei and total MMP9 present after 2 hour treatment with heme and iron. TNF-α was used as a positive control and no change was observed, suggesting that in this model increases in MMP9 expression are only detectable at the mRNA level. The images demonstrate that there was no observable difference in the level of MMP9 detected between the heme and iron treatments with the control. This could indicate that the time point investigated was too soon to notice differences in MMP9 protein levels or that the regulation of MMP9 by heme and iron treatment may only occur at the transcriptional level.

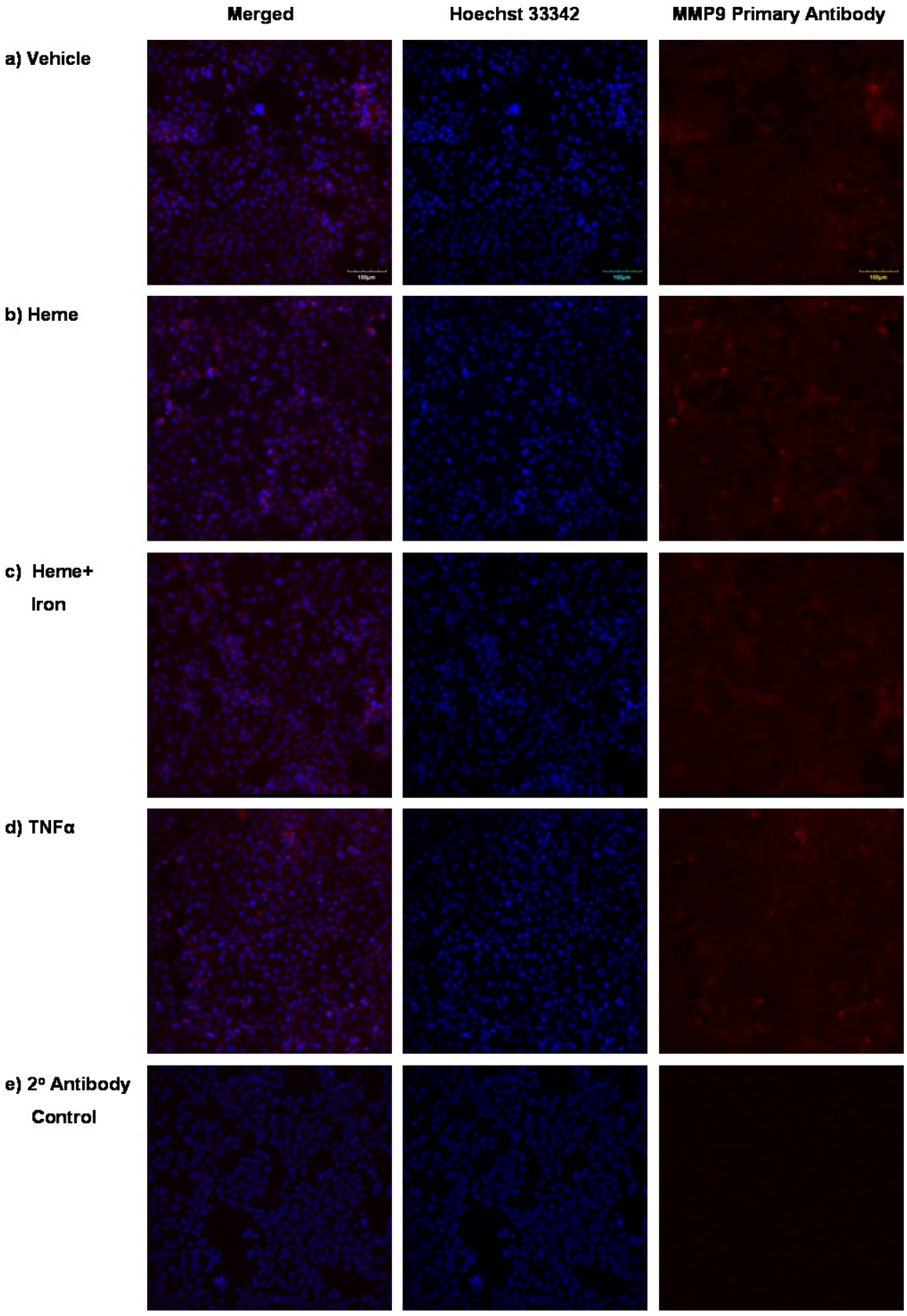
Merged
Hoechst 33342
MMP9 Primary Antibody
a) Vehicle
b) Heme
c) Heme+ Iron
d) TNFα
e) 2º Antibody Control

Figure 11: Immunofluorescence to detect the levels of MMP9 protein in NRA cells: Immunofluorescence shows MMP9 protein in NRA cells treated with a) vehicle (7.6 mM NaOH), b) 40μM hemin chloride, c) 40 μM hemin chloride and 50μM iron (II) sulfate, and d) TNFα 40 ng/ml. Image e) is the secondary control to show that there was no non-specific binding of the secondary antibody. The cells were stained with Hoechst 33342 to visualize nuclei (blue) and a primary MMP9 antibody (red). Images were taken at 20X magnification and the scale bar is shown in image a) and represents 100μm.

CHAPTER 4: DISCUSSION

Blood-brain barrier disruption is one of the main causes of cerebral damage following cerebral ischemia and hemorrhage. MMP9 has been characterized as the main protease responsible for the sustained opening of the BBB (Rosenberg GA et al. 1998) resulting in cell death, edema, infiltration of inflammatory cells, and secondary brain damage. While MMP9 has been identified as the main mediator of BBB disruption, the signaling pathways involved in its expression have not been fully elucidated.

In the present study my work has demonstrated that the expression of MMP9 at the mRNA level occurs following the deposition of heme and iron in rat astrocytes (NRA cells), identifying another stimulus responsible for up-regulating MMP9 expression following ischemic stroke and hemorrhage. My work also showed that heme and iron generated ROS, which may be the mechanism in which AP-1 and NFκB signaling pathways are activated. This study also demonstrated that inhibiting these pathways resulted in the decreased expression of MMP9. Lastly, I have demonstrated that the heme and iron stimulated the increased expression of HO-1 by activating the transcription factor Nrf2. All together, the results of this study help provide a better understanding of the signaling pathways involved in heme and iron induced MMP9 expression which may occur following cerebral ischemia and hemorrhage.

4.1 Heme and Iron Induce MMP9 Expression

In this study an *in vitro* NRA cell model was used and heme and iron were exogenously added to the media and cells in order to mimic their deposition within the brain on neural cells following hemorrhage. It was demonstrated that MMP9 gene expression was upregulated at the mRNA levels by the heme and iron treatment in this model following 2 hours of treatment and that the levels return to baseline at 8 hours (Figure 5A). Many studies have shown that MMP9 expression is increased following ischemic stroke by various stimuli, such as inflammatory cytokines (Denes A et al. 2010) and ROS (Malcolmson E 2011). Demonstrating that heme and iron treatment caused an increase in MMP9 gene expression provides insight into another stimulus that may potentiate BBB breakdown by increasing the expression of MMP9 following stroke.

In order to characterize the mechanism of heme/iron-mediated upregulation of MMP9, I have assayed whether heme and iron can generate ROS, a known stimulus of MMP9 expression. Figure 7 shows that treatment of cells with heme and iron generated significant amounts of ROS as compared to vehicle and control. This is most likely the major mechanism responsible for the observed increase in MMP9 in this model. Studies using a ROS scavenger would demonstrate whether the generated ROS, by heme and iron, is the main mechanism for the observed increase in MMP9 expression. Heme and iron may have a direct effect on activating these signaling pathways or on up-regulating MMP9 expression, but these still needs to be investigated.

MMP9 protein expression was found to be unchanged following 2 and 8 hours of treatment with heme and iron in the present study (Figure 10). This observation may be due to the model or the time point observed, but a more likely explanation is that post-transcriptional modifications are occurring resulting in the mRNA not being translated to protein. Previous work has shown that MMP9 is present within 24 hours following MCAO in rats (Zhao BQ et al. 2006). A previous *In vitro* study in our laboratory showed increases in active MMP9 protein levels at 6 hours in NRA cells treated with a strong stimulus hydrogen peroxide (Malcolmson E 2011). A study by Ralay Ranaivo and colleagues demonstrated an increase in MMP9 expression and activity after 24 hours of albumin treatment in rat astrocytes (Ralay Ranaivo H et al. 2012).

4.2 Signaling Pathways Involved in Heme and Iron Induced MMP9 Expression

In the present study I have demonstrated that the transcription factors AP-1 and NFκB are activated following heme and iron treatment in cells (Figure 6). I have also demonstrated that the inhibition of JNK resulted in the decreased expression of MMP9 (Figure 8A). As well, inhibition of IKK activation or the proteosome resulted in the reduction of MMP9 expression following heme and iron treatment (Figure 8B and C). Previous work has identified multiple signaling pathways as being responsible for increased MMP9 expression by the activation of different stimuli. Wu and colleagues demonstrated that stimulation of RBA-1 cells by IL-1β resulted in increased expression of MMP9 through the activation of MAPK and NFκB (Wu CY et al. 2004). It was also shown that the MAPK and NFκB activation occurs in human alveolar epithelial cell

carcinoma by IL-1β stimulation (Lin CC et al. 2009). Wang and colleagues showed that oxidized low-density lipoprotein caused an increase in MMP9 expression in rat brain astrocytes by a p42/p44 (MAPK) and JNK-dependent AP-1 signaling pathway (Wang HH et al. 2009). Oxygen deprivation has also been shown to induce the MAPK, ERK1/2 in cortical neurons (Boulous S et al. 2007). And it was shown that inhibition of ERK1/2 in rat astrocytes results in the reduction of MMP9 expression after PMA stimulation (Arai K et al. 2003). MMP9 expression is also stimulated by TNFα through the activation of NFκB (Hozumi A et al. 2001, Itatsu K et al. 2009). TNFα also induces MMP9 expression through the phosphorylation of ERK1/2 and p38 MAPK (Itatsu et al. 2009). Lastly, TNFα has been shown to stimulate other pathways involved in MMP9 upregulation, including the PI3K/Akt signaling pathway (Hwang MK et al. 2009). Taken together these results demonstrate the complexity of MMP9 expression mechanisms that can occur under different conditions. However, it was unknown whether heme and iron deposited in the brain following cerebral ischemia and hemorrhage would play a role in regulating MMP9 expression. My data presented here has demonstrated that both heme and iron deposited on astrocytes of this *in vitro* model can generate ROS, activate AP-1 and NFκB signaling pathways and upregulate MMP9 expression, implicating that heme and iron deposition in the brain following ischemic stroke and hemorrhage may play a role in modulating MMP9 expression.

4.3 Role of Heme Oxygenase-1 and Nrf2

Heme oxygenase-1 is the rate-limiting enzyme involved in the degradation of heme into biliverdin and CO (Wang J and Doré S 2007; Wang J and Doré S 2008). In the

present study HO-1 expression was found to be increased following treatment with heme and iron at 4 hours, with the expression remaining increased up to 8 hours (Figure 5B). The role of HO-1 is to protect the cell from the toxicity of heme by breaking it down and allowing for the sequestering of Fe^{2+} protecting the cell from free radicals produced by the iron. Studies have demonstrated that HO-1 is protective against oxidative injury in mouse astrocytes (Chen- Roetling J et al. 2005) and that it can protect against hemin (Benvenisti-Zarom L and Regan RF 2007; Chen J and Regan RF 2005; Teng ZP et al. 2004). In the present study the increase in HO-1 expression was observed at the gene level and whether the expression of the HO-1 protein is also upregulated needs to be investigated. Upregulation of heme oxygenase-1 expression is known to be mediated by the Nrf2.

The activation of Nrf2 occurs in response to oxidative stress and is responsible for the transcription of many antioxidant enzymes (Kensler TW et al. 2007). In the present study the activation of Nrf2 was found to occur after 2 hours of treatment with heme and iron (Figure 6C). This result was expected since there was significant ROS produced by the treatment (Figure 7) and activated Nrf2 is also responsible for HO-1 expression. Many studies have identified Nrf2 as being potentially neuroprotective. In a mouse model of intracerebral hemorrhage (ICH) it was found that the knockdown of Nrf2 resulted in greater injury and increased neurological deficits (Wang J et al. 2007). Another study showed that sulphorane-activated Nrf2 protected against oxidative damage and neurological deficits in a rat model of ICH (Zhoa X et al. 2007). Additionally, it was demonstrated that the knockout of Nrf2 resulted in increased MMP9 expression, and neuroinflammation in rat primary astrocytes treated with oxyhemoglobin (Pan H et al.

2011). The activation of Nrf2 by heme and iron deposition is a protective response by the cell when treated by the heme and generated ROS and may play an important role in preventing injury following cerebral ischemia and hemorrhage since it has been identified as neuroprotective.

4.4 Conclusion and Future Direction

Heme and iron are deposited at the site of brain injury during hemorrhagic and/or ischemic stroke or following tPA treatment. The present study has demonstrated that this deposition can result in the increased expression of MMP9 in the *in vitro* model of rat astrocytes. I have shown that heme and iron deposition generates ROS and activates the transcription factors AP-1 and NFκB which are responsible for the observed increase in MMP9 expression. Inhibition of the upstream kinase of AP-1 signaling pathway, JNK, prevented the increase in MMP9 expression. Similarly, inhibition of the activation of IKK or the proteosome (to prevent IκB-α degradation) for NFκB signaling pathway also resulted in the prevention of MMP9 upregulation stimulated by heme and iron. These results suggest that targeting the generation of ROS and the activation of the AP-1 and NFκB signaling pathways may be beneficial in modulating MMP9 expression and in relieving MMP9-mediated BBB disruption. However, MMP9 is also needed for brain repair and angiogenesis following brain injury. Thus, spatial modulation of MMP9 expression at different stages of brain injury and recovery will be crucial for limiting the damage at the early stage and promoting a better and faster recovery at the late stage. My study has demonstrated that Nrf2 is activated following heme and iron deposition in astrocytes and that it results in increased expression of HO-1. As suggest in the

literature, the activation of Nrf2 and expression of HO-1 are potentially neuroprotective. Further studies should be conducted to better understand spatial regulation of MMP9 following heme and iron deposition at different stages in *in vivo* models and to understand the role of Nrf2 in protecting against oxidative stress and whether Nrf2 expression is protective against MMP9-induced BBB disruption.

REFERENCES

Abbott NJ, Patabendige AA, Dolman DE, Yusof SR, Begley DJ. (2010). **Structure and function of the blood-brain barrier**. Neurobiol Dis, 37(1),13-25.

Abbott NJ, Rönnbäck L, Hansson E. (2006). **Astrocyte-endothelial interactions at the blood-brain barrier**. Nat Rev Neurosci, 7(1), 41-53.

Abraham NG, Kappas A. (2005). **Heme oxygenase and the cardiovascular-renal system**. Free Radic Biol Med, 39(1), 1-25.

Adibhatla RM, Hatcher JF. (2008). **Tissue plasminogen activator (tPA) and matrix metalloproteinases in the pathogenesis of stroke: therapeutic strategies**. CNS Neurol Disord Drug Targets, 7(3), 243-53.

Arai K, Lee SR, Lo EH. (2003). **Essential role for ERK mitogen-activated protein kinase in matrix metalloproteinase-9 regulation in rat cortical astrocytes.** Glia, 43(3), 254-64.

Armulik A, Abramsson A, Betsholtz C. (2005). **Endothelial/pericyte interactions**. Circ Res, 97(6), 512-23.

Aronowski J, Zhao X. (2011). **Molecular pathophysiology of cerebral hemorrhage: secondary brain injury**. Stroke, 42(6), 1781-6.

Asahi M, Wang X, Mori T, Sumii T, Jung JC, Moskowitz MA, Fini ME, Lo EH. (2001). **Effects of matrix metalloproteinase-9 gene knock-out on the proteolysis of blood-brain barrier and white matter components after cerebral ischemia**. J Neurosci, 21(19), 7724-32.

Benvenisti-Zarom L, Regan RF. (2007). **Astrocyte-specific heme oxygenase-1 hyperexpression attenuates heme-mediated oxidative injury**. Neurobiol Dis, 26(3), 688-95.

Blasi P, Giovagnoli S, Schoubben A, Ricci M, Rossi C. (2007) **Solid lipid nanoparticles for targeted brain drug delivery**. Adv Drug Deliv Rev, 59(6), 454-77.

Boulos S, Meloni BP, Arthur PG, Majda B, Bojarski C, Knuckey NW. (2007). **Evidence that intracellular cyclophilin A and cyclophilin A/CD147 receptor-mediated ERK1/2 signalling can protect neurons against in vitro oxidative and ischemic injury**. Neurobiol Dis, 25(1),54-64.

Brew K, Dinakarpandian D, Nagase H. (2000). **Tissue inhibitors of metalloproteinases: evolution, structure and function**. Biochim Biophys Acta, 1477(1-2), 267-83.

Candelario-Jalil E, Taheri S, Yang Y, Sood R, Grossetete M, Estrada EY, Fiebich BL, Rosenberg GA. (2007). **Cyclooxygenase inhibition limits blood-brain barrier disruption following intracerebral injection of tumor necrosis factor-alpha in the rat**. J Pharmacol Exp Ther, 323(2), 488-98.

Cecchelli R, Berezowski V, Lundquist S, Culot M, Renftel M, Dehouck MP, Fenart L. (2007). **Modelling of the blood-brain barrier in drug discovery and development**. Nat Rev Drug Discov, 6(8), 650-61.

Chen J, Regan RF. (2005). **Increasing expression of heme oxygenase-1 by proteasome inhibition protects astrocytes from heme-mediated oxidative injury**. Curr Neurovasc Res, 2(3), 189-96.

Chen W, Hartman R, Ayer R, Marcantonio S, Kamper J, Tang J, Zhang JH. (2009). **Matrix metalloproteinases inhibition provides neuroprotection against hypoxia-ischemia in the developing brain**. J Neurochem, 111(3), 726-36.

Chen Y, Hallenbeck JM, Ruetzler C, Bol D, Thomas K, Berman NE, Vogel SN. (2003). **Overexpression of monocyte chemoattractant protein 1 in the brain exacerbates ischemic brain injury and is associated with recruitment of inflammatory cells**. J Cereb Blood Flow Metab, 23(6), 748-55.

Chen-Roetling J, Benvenisti-Zarom L, Regan RF. (2005). **Cultured astrocytes from heme oxygenase-1 knockout mice are more vulnerable to heme-mediated oxidative injury**. J Neurosci Res, 82(6), 802-10.

Collier IE, Krasnov PA, Strongin AY, Birkedal-Hansen H, Goldberg GI. (1992). **Alanine scanning mutagenesis and functional analysis of the fibronectin-like collagen-binding domain from human 92-kDa type IV collagenase**. J Biol Chem, 267(10), 6776-81.

Crocker SJ, Milner R, Pham-Mitchell N, Campbell IL. (2006). **Cell and agonist-specific regulation of genes for matrix metalloproteinases and their tissue inhibitors by primary glial cells**. J Neurochem, 98(3), 812-23.

Cunningham LA, Wetzel M, Rosenberg GA. (2005). **Multiple roles for MMPs and TIMPs in cerebral ischemia**. Glia, 50(4), 329-39.

Dang TN, Bishop GM, Dringen R, Robinson SR. (2010). **The putative heme transporter HCP1 is expressed in cultured astrocytes and contributes to the uptake of hemin**. Glia, 58(1), 55-65.

Denes A, Thornton P, Rothwell NJ, Allan SM. (2010). **Inflammation and brain injury: acute cerebral ischaemia, peripheral and central inflammation**. Brain Behav Immun, 24(5), 708-23.

Elkins PA, Ho YS, Smith WW, Janson CA, D'Alessio KJ, McQueney MS, Cummings MD, Romanic AM. (2002). **Structure of the C-terminally truncated human ProMMP9, a gelatin-binding matrix metalloproteinase**. Acta Crystallogr D Biol Crystallogr, 58(Pt 7), 1182-92.

Fujimoto M, Takagi Y, Aoki T, Hayase M, Marumo T, Gomi M, Nishimura M, Kataoka H, Hashimoto N, Nozaki K. (2008). **Tissue inhibitor of metalloproteinases protect blood-brain barrier disruption in focal cerebral ischemia**. J Cereb Blood Flow Metab, 28(10), 1674-85.

Gidday JM, Gasche YG, Copin JC, Shah AR, Perez RS, Shapiro SD, Chan PH, Park TS. (2005). **Leukocyte-derived matrix metalloproteinase-9 mediates blood-brain barrier breakdown and is proinflammatory after transient focal cerebral ischemia**. Am J Physiol Heart Circ Physiol, 289(2), H558-68.

Gilgun-Sherki Y, Melamed E, Offen D. (2001). **Oxidative stress induced-neurodegenerative diseases: the need for antioxidants that penetrate the blood brain barrier**. Neuropharmacology, 40(8), 959-75.

Gorman AM, McGowan A, O'Neill C, Cotter T. (1996). **Oxidative stress and apoptosis in neurodegeneration**. J Neurol Sci, 139 Suppl, 45-52.

Gottschall PE, Yu X. (1995). **Cytokines regulate gelatinase A and B (matrix metalloproteinase 2 and 9) activity in cultured rat astrocytes**. J Neurochem, 64(4), 1513-20.

Gu Z, Kaul M, Yan B, Kridel SJ, Cui J, Strongin A, Smith JW, Liddington RC, Lipton SA. (2002). **S-nitrosylation of matrix metalloproteinases: signaling pathway to neuronal cell death**. Science, 297(5584), 1186-90.

Holvoet S, Vincent C, Schmitt D, Serres M. (2003). **The inhibition of MAPK pathway is correlated with down-regulation of MMP-9 secretion induced by TNF-alpha in human keratinocytes**. Exp Cell Res, 290(1), 108-19.

Hozumi A, Nishimura Y, Nishiuma T, Kotani Y, Yokoyama M. (2001). **Induction of MMP-9 in normal human bronchial epithelial cells by TNF-alpha via NF-kappa B-mediated pathway**. Am J Physiol Lung Cell Mol Physiol, 281(6), L1444-52.

Hu Q, Chen C, Khatibi NH, Li L, Yang L, Wang K, Han J, Duan W, Zhang JH, Zhou C. (2011). **Lentivirus-mediated transfer of MMP-9 shRNA provides neuroprotection following focal ischemic brain injury in rats**. Brain Res, 1367, 347-59.

Huang CY, Fujimura M, Chang YY, Chan PH. (2001a) **Overexpression of copper-zinc superoxide dismutase attenuates acute activation of activator protein-1 after transient focal cerebral ischemia in mice**. Stroke, 32(3), 741-7.

Huang CY, Fujimura M, Noshita N, Chang YY, Chan PH. (2001b). **SOD1 down-regulates NF-kappaB and c-Myc expression in mice after transient focal cerebral ischemia**. J Cereb Blood Flow Metab, 21(2), 163-73.

Hwang MK, Song NR, Kang NJ, Lee KW, Lee HJ. (2009). **Activation of phosphatidylinositol 3-kinase is required for tumor necrosis factor-alpha-induced upregulation of matrix metalloproteinase-9: its direct inhibition by quercetin**. Int J Biochem Cell Biol, 41(7), 1592-600.

Itatsu K, Sasaki M, Harada K, Yamaguchi J, Ikeda H, Sato Y, Ohta T, Sato H, Nagino M, Nimura Y, Nakanuma Y. (2009). **Phosphorylation of extracellular signal-regulated kinase 1/2, p38 mitogen-activated protein kinase and nuclear translocation of nuclear factor-kappaB are involved in upregulation of matrix metalloproteinase-9 by tumour necrosis factor-alpha**. Liver Int, 29(2), 291-8.

Jeney V, Balla J, Yachie A, Varga Z, Vercellotti GM, Eaton JW, Balla G. (2002) **Pro-oxidant and cytotoxic effects of circulating heme**. Blood, 100(3), 879–887.

Juurlink BH, Sweeney MI. (1997). **Mechanisms that result in damage during and following cerebral ischemia**. Neurosci Biobehav Rev, 21(2), 121-8.

Katsu M, Niizuma K, Yoshioka H, Okami N, Sakata H, Chan PH. (2010). **Hemoglobin-induced oxidative stress contributes to matrix metalloproteinase activation and blood-brain barrier dysfunction in vivo**. J Cereb Blood Flow Metab, 30(12), 1939-50.

Kauppinen TM, Swanson RA. (2005). **Poly(ADP-ribose) polymerase-1 promotes microglial activation, proliferation, and matrix metalloproteinase-9-mediated neuron death**. J Immunol, 174(4), 2288-96.

Kensler TW, Wakabayashi N, Biswal S. (2007). **Cell survival responses to environmental stresses via the Keap1-Nrf2-ARE pathway**. Annu Rev Pharmacol Toxicol, 47, 89-116.

Kim GW, Gasche Y, Grzeschik S, Copin JC, Maier CM, Chan PH. (2003). **Neurodegeneration in striatum induced by the mitochondrial toxin 3-nitropropionic acid: role of matrix metalloproteinase-9 in early blood-brain barrier disruption?** J Neurosci, 23(25), 8733-42.

Kim SI, Kim HJ, Han DC, Lee HB. (2000). **Effect of lovastatin on small GTP binding proteins and on TGF-beta1 and fibronectin expression**. Kidney Int Suppl, 77, S88-92.

Koeppen AH, Dickson AC, Smith J. (2004). **Heme oxygenase in experimental intracerebral hemorrhage: the benefit of tin-mesoporphyrin**. J Neuropathol Exp Neurol, 63(6), 587-97.

Lakhan SE, Kirchgessner A, Hofer M. (2009). **Inflammatory mechanisms in ischemic stroke: therapeutic approaches**. J Transl Med, 7, 97.

Lara FA, Kahn SA, da Fonseca AC, Bahia CP, Pinho JP, Graca-Souza AV, Houzel JC, de Oliveira PL, Moura-Neto V, Oliveira MF. (2009). **On the fate of extracellular hemoglobin and heme in brain**. J Cereb Blood Flow Metab, 29(6), 1109-20.

Lee J, Rhee MH, Kim E, Cho JY. (2012). **BAY 11-7082 Is a Broad-Spectrum Inhibitor with Anti-Inflammatory Activity against Multiple Targets**. Mediators Inflamm, 2012, 416036.

Lee SR, Guo SZ, Scannevin RH, Magliaro BC, Rhodes KJ, Wang X, Lo EH. (2007). **Induction of matrix metalloproteinase, cytokines and chemokines in rat cortical astrocytes exposed to plasminogen activators**. Neurosci Lett, 417(1),1-5.

Lee SR, Tsuji K, Lee SR, Lo EH. (2004). **Role of matrix metalloproteinases in delayed neuronal damage after transient global cerebral ischemia**. J Neurosci, 24(3), 671-8.

Levicar N, Nuttall RK, Lah TT. (2003). **Proteases in brain tumour progression**. Acta Neurochir (Wien), 145(9), 825-38.

Lin CC, Kuo CT, Cheng CY, Wu CY, Lee CW, Hsieh HL, Lee IT, Yang CM. (2009). **IL-1 beta promotes A549 cell migration via MAPKs/AP-1- and NF-kappaB-dependent matrix metalloproteinase-9 expression**. Cell Signal, 21(11), 1652-62.

Lv S, Song HL, Zhou Y, Li LX, Cui W, Wang W, Liu P. (2010). **Tumour necrosis factor-alpha affects blood-brain barrier permeability and tight junction-associated occludin in acute liver failure**. Liver Int, 30(8), 1198-210.

Maddahi A, Chen Q, Edvinsson L. (2009). **Enhanced cerebrovascular expression of matrix metalloproteinase-9 and tissue inhibitor of metalloproteinase-1 via the MEK/ERK pathway during cerebral ischemia in the rat**. BMC Neurosci, 10, 56.

Malcolmson E. **Reactive Oxygen Species (ROS) up-regulates MMP-9 expression via MAPK-AP1 signaling pathway in rat astrocytes** [Master's Thesis]. [Ottawa (ON)]: University of Ottawa; 2011. 108 p.

Mao L, Wang H, Qiao L, Wang X. (2010). **Disruption of Nrf2 enhances the upregulation of nuclear factor-kappaB activity, tumor necrosis factor-α, and matrix metalloproteinase-9 after spinal cord injury in mice**. Mediators Inflamm. 2010, 238321.

Matz, P.G., P.R. Weinstein & F.R. Sharp. (1997). **Heme oxygenase-1 and heat shock protein 70 induction in glia and neurons throughout rat brain after experimental intracerebral hemorrhage**. Neurosurgery, 40, 152–160.

Morgunova E, Tuuttila A, Bergmann U, Isupov M, Lindqvist Y, Schneider G, Tryggvason K. (1999). **Structure of human pro-matrix metalloproteinase-2: activation mechanism revealed**. Science, 284(5420), 1667-70.

Morita-Fujimura Y, Fujimura M, Gasche Y, Copin JC, Chan PH. (2000). **Overexpression of copper and zinc superoxide dismutase in transgenic mice prevents the induction and activation of matrix metalloproteinases after cold injury-induced brain trauma**. J Cereb Blood Flow Metab, 20(1), 130-8.

Negi G, Kumar A, Joshi RP, Sharma SS. (2011). **Oxidative stress and Nrf2 in the pathophysiology of diabetic neuropathy: old perspective with a new angle**. Biochem Biophys Res Commun, 408(1), 1-5.

Pan H, Wang H, Zhu L, Mao L, Qiao L, Su X. (2011). **Depletion of Nrf2 enhances inflammation induced by oxyhemoglobin in cultured mice astrocytes**. Neurochem Res, 36(12), 2434-41.

Persidsky Y, Ramirez SH, Haorah J, Kanmogne GD. (2006). **Blood-brain barrier: structural components and function under physiologic and pathologic conditions**. J Neuroimmune Pharmacol, 1(3), 223-36.

Pfefferkorn T, Rosenberg GA. (2003). **Closure of the blood-brain barrier by matrix metalloproteinase inhibition reduces rtPA-mediated mortality in cerebral ischemia with delayed reperfusion**. Stroke, 34(8), 2025-30.

Rajagopalan S, Meng XP, Ramasamy S, Harrison DG, Galis ZS. (1996). **Reactive oxygen species produced by macrophage-derived foam cells regulate the activity of vascular matrix metalloproteinases in vitro**. **Implications for atherosclerotic plaque stability.** J Clin Invest, 98(11), 2572-9.

Ralay Ranaivo H, Hodge JN, Choi N, Wainwright MS. (2012). **Albumin induces upregulation of matrix metalloproteinase-9 in astrocytes via MAPK and reactive oxygen species-dependent pathways**. J Neuroinflammation, 9, 68.

Ram M, Sherer Y, Shoenfeld Y. (2006). **Matrix metalloproteinase-9 and autoimmune diseases**. J Clin Immunol. 26(4), 299-307.

Rosell A, Cuadrado E, Ortega-Aznar A, Hernández-Guillamon M, Lo EH, Montaner J. (2008) **MMP-9-positive neutrophil infiltration is associated to blood-brain barrier breakdown and basal lamina type IV collagen degradation during hemorrhagic transformation after human ischemic stroke**. Stroke, 39(4), 1121-6.

Rosenberg GA, Estrada EY, Dencoff JE. (1998). **Matrix metalloproteinases and TIMPs are associated with blood-brain barrier opening after reperfusion in rat brain**. Stroke, 29(10), 2189-95.

Rosenberg GA, Estrada EY, Dencoff JE, Stetler-Stevenson WG. (1995). **Tumor necrosis factor-alpha-induced gelatinase B causes delayed opening of the blood-brain barrier: an expanded therapeutic window**. Brain Res, 703(1-2), 151-5.

Sandoval KE, Witt KA. (2008). **Blood-brain barrier tight junction permeability and ischemic stroke**. Neurobiol Dis, 32(2), 200-19.

Simonian NA, Coyle JT. (1996). **Oxidative stress in neurodegenerative diseases**. Annu Rev Pharmacol Toxicol, 36, 83-106.

Sternlicht MD, Werb Z. (2001). **How matrix metalloproteinases regulate cell behavior**. Annu Rev Cell Dev Biol, 17, 463-516.

Suofu Y, Clark JF, Broderick JP, Kurosawa Y, Wagner KR, Lu A. (2012). **Matrix metalloproteinase-2 or -9 deletions protect against hemorrhagic transformation during early stage of cerebral ischemia and reperfusion**. Neuroscience, 212, 180-9.

Tang CH, Tsai CC. (2012). **CCL2 increases MMP-9 expression and cell motility in human chondrosarcoma cells via the Ras/Raf/MEK/ERK/NF-κB signaling pathway**. Biochem Pharmacol, 83(3), 335-44.

Tao-Cheng JH, Brightman MW. (1988). **Development of membrane interactions between brain endothelial cells and astrocytes in vitro**. Int J Dev Neurosci, 6(1), 25-37.

Teng ZP, Chen J, Chau LY, Galunic N, Regan RF. (2004). **Adenoviral transfer of the heme oxygenase-1 gene protects striatal astrocytes from heme-mediated oxidative injury**. Neurobiol Dis, 17(2), 179-87.

Tochowicz A, Maskos K, Huber R, Oltenfreiter R, Dive V, Yiotakis A, Zanda M, Pourmotabbed T, Bode W, Goettig P. (2007). **Crystal structures of MMP-9 complexes with five inhibitors: contribution of the flexible Arg424 side-chain to selectivity**. J Mol Biol, 371(4), 989-1006.

Tsuge M, Yasui K, Ichiyawa T, Saito Y, Nagaoka Y, Yashiro M, Yamashita N, Morishima T. (2010). **Increase of tumor necrosis factor-alpha in the blood induces early activation of matrix metalloproteinase-9 in the brain**. Microbiol Immunol, 54(7), 417-24.

Wagener FA, Eggert A, Boerman OC, Oyen WJ, Verhofstad A, Abraham NG, Adema G, van Kooyk Y, de Witte T, Figdor CG. (2001). **Heme is a potent inducer of inflammation in mice and is counteracted by heme oxygenase**. Blood, 98(6), 1802-11.

Wakisaka Y, Chu Y, Miller JD, Rosenberg GA, Heistad DD. (2010). **Critical role for copper/zinc-superoxide dismutase in preventing spontaneous intracerebral hemorrhage during acute and chronic hypertension in mice**. Stroke, 41(4), 790-7.

Wang HH, Hsieh HL, Wu CY, Sun CC, Yang CM. (2009). **Oxidized low-density lipoprotein induces matrix metalloproteinase-9 expression via a p42/p44 and JNK-dependent AP-1 pathway in brain astrocytes**. Glia, 57(1), 24-38.

Wang J, Doré S. (2008). **Heme oxygenase 2 deficiency increases brain swelling and inflammation after intracerebral hemorrhage**. Neuroscience, 155(4), 1133-41.

Wang J, Doré S. (2007). **Heme oxygenase-1 exacerbates early brain injury after intracerebral haemorrhage**. Brain, 130(Pt 6), 1643-52

Wang J, Fields J, Zhao C, Langer J, Thimmulappa RK, Kensler TW, Yamamoto M, Biswal S, Doré S. (2007). **Role of Nrf2 in protection against intracerebral hemorrhage injury in mice**. Free Radic Biol Med, 43(3), 408-14.

Wang X, Jung J, Asahi M, Chwang W, Russo L, Moskowitz MA, Dixon CE, Fini ME, Lo EH. (2000). **Effects of matrix metalloproteinase-9 gene knock-out on morphological and motor outcomes after traumatic brain injury**. J Neurosci, 20(18). 7037-42.

Williamson RA, Marston FA, Angal S, Koklitis P, Panico M, Morris HR, Carne AF, Smith BJ, Harris TJ, Freedman RB. (1990). **Disulphide bond assignment in human tissue inhibitor of metalloproteinases (TIMP)**. Biochem J, 268(2), 267-74.

Wu CY, Hsieh HL, Jou MJ, Yang CM. (2004). **Involvement of p42/p44 MAPK, p38 MAPK, JNK and nuclear factor-kappa B in interleukin-1beta-induced matrix metalloproteinase-9 expression in rat brain astrocytes**. J Neurochem, 90(6), 1477-88.

Xi, G., R.F. Keep & J.T. Hoff. (1998). **Erythrocytes and delayed brain edema formation following intracerebral hemorrhage in rats**. J. Neurosurg, 89: 991–996.

Xu X, Chen Z, Wang Y, Yamada Y, Steffensen B. (2005). **Functional basis for the overlap in ligand interactions and substrate specificities of matrix metalloproteinases-9 and -2**. Biochem J, 392(Pt 1), 127-34.

Yang Y, Rosenberg GA. (2011a). **Blood-brain barrier breakdown in acute and chronic cerebrovascular disease**. Stroke, 42(11), 3323-8.

Yang Y, Rosenberg GA. (2011b). **MMP-mediated disruption of claudin-5 in the blood-brain barrier of rat brain after cerebral ischemia**. Methods Mol Biol, 762, 333-45.

Yang Y, Estrada EY, Thompson JF, Liu W, Rosenberg GA. (2007). **Matrix metalloproteinase-mediated disruption of tight junction proteins in cerebral vessels is reversed by synthetic matrix metalloproteinase inhibitor in focal ischemia in rat**. J Cereb Blood Flow Metab, 27(4), 697-709.

Zhao J, Moore AN, Redell JB, Dash PK. (2007). **Enhancing expression of Nrf2-driven genes protects the blood brain barrier after brain injury**. J Neurosci, 27(38), 10240-8.

Zhao BQ, Wang S, Kim HY, Storrie H, Rosen BR, Mooney DJ, Wang X, Lo EH. (2006). **Role of matrix metalloproteinases in delayed cortical responses after stroke**. Nat Med, 12(4), 441-5.

Zhao X, Sun G, Zhang J, Strong R, Dash PK, Kan YW, Grotta JC, Aronowski J. (2007) **Transcription factor Nrf2 protects the brain from damage produced by intracerebral hemorrhage**. Stroke, 38(12), 3280-6.

Zlokovic BV. (2008). **The blood-brain barrier in health and chronic neurodegenerative disorders**. Neuron, 57(2), 178-201.